

Review

# A Short Review of Advancements in Additive Manufacturing of Cemented Carbides

Zhe Zhao <sup>1</sup>, Xiaonan Ni <sup>1</sup>, Zijian Hu <sup>1</sup>, Wenxin Yang <sup>1</sup>, Xin Deng <sup>1,2,\*</sup>, Shanghua Wu <sup>1,2</sup>, Yanhui Li <sup>1,2</sup>, Guanglin Nie <sup>2,\*</sup>, Haidong Wu <sup>1,2</sup>, Jinyang Liu <sup>1,2</sup> and Yong Huang <sup>3</sup>

- <sup>1</sup> Department of Mechanical Design, Manufacturing and Automation, School of Electromechanical Engineering, Guangdong University of Technology, Guangzhou 510006, China; zhezhaogdut.edu.cn (Z.Z.); 1112201040@mail2.gdut.edu.cn (X.N.); 1112101029@mail2.gdut.edu.cn (Z.H.); 1112201021@mail2.gdut.edu.cn (W.Y.); swu@gdut.edu.cn (S.W.); lyhklyg@163.com (Y.L.); whd1152967796@163.com (H.W.); 18904044272@163.com (J.L.)
- <sup>2</sup> Guangdong Metal Ceramic 3D Technology Co., Ltd., Foshan 528216, China
- <sup>3</sup> Guangzhou Dopo Scientific Instrument Co., Ltd., Guangzhou 510555, China; 18922239889@189.cn
- \* Correspondence: dengxin@gdut.edu.cn (X.D.); buildingmaterials8@163.com (G.N.)

**Abstract:** Cemented carbides, renowned for their exceptional strength, hardness, elastic modulus, wear resistance, corrosion resistance, low coefficient of thermal expansion, and chemical stability, have long been indispensable tooling materials in metal cutting, oil drilling, and engineering excavation. The advent of additive manufacturing (AM), commonly known as “3D printing”, has sparked considerable interest in the processing of cemented carbides. Among the various AM techniques, Selective Laser Melting (SLM), Selective Laser Sintering (SLS), Selective Electron Beam Melting (SEBM), and Binder Jetting Additive Manufacturing (BJAM) have garnered frequent attention. Despite the great application potential of AM, no single AM technique has been universally adopted for the large-scale production of cemented carbides yet. The SLM and SEBM processes confront substantial challenges, such as a non-uniform sintering temperature field, which often result in uneven sintering and frequent post-solidification cracking. SLS notably struggles with achieving a high relative density of carbides. While BJAM yields WC-Co samples with a lower incidence of cracking, it is not without flaws, including abnormal WC grain growth, coarse WC clustering, Co-rich pool formation, and porosity. Three-dimensional gel-printing, though possessing certain advantages from its sintering performance, falls short in dimensional and geometric precision control, as well as fabrication efficiency. Cemented carbides produced via AM processes have yet to match the quality of their traditionally prepared counterparts. To date, the specific densification and microstructure evolution mechanisms during the AM process, and their interrelationship with the feedstock carbide material design, printing/sintering process, and resulting mechanical behavior, have not been thoroughly investigated. This gap in our knowledge impedes the rapid advancement of AM for carbide processing. This article offers a succinct overview of additive manufacturing of cemented carbides, complemented by an analysis of the current research landscape. It highlights the benefits and inherent challenges of these techniques, aiming to provide clarity on the present state of the AM processing of cemented carbides and to offer insights into potential future research directions and technological advancements.



Academic Editor: Marek Sroka

Received: 28 December 2024

Revised: 21 January 2025

Accepted: 27 January 2025

Published: 30 January 2025

**Citation:** Zhao, Z.; Ni, X.; Hu, Z.; Yang, W.; Deng, X.; Wu, S.; Li, Y.; Nie, G.; Wu, H.; Liu, J.; et al. A Short Review of Advancements in Additive Manufacturing of Cemented Carbides. *Crystals* **2025**, *15*, 146. <https://doi.org/10.3390/cryst15020146>

**Copyright:** © 2025 by the authors. Licensee MDPI, Basel, Switzerland. This article is an open access article distributed under the terms and conditions of the Creative Commons Attribution (CC BY) license (<https://creativecommons.org/licenses/by/4.0/>).

**Keywords:** cemented carbide; additive manufacturing; microstructure; mechanical properties; experimental techniques

## 1. Introduction

Cemented carbides, renowned for their exceptional properties, such as high strength, hardness, and wear resistance, have become the material of choice for cutting tools. They are extensively used in the manufacturing of turning blades, drill bits, and saw heads for a variety of materials, including metals, concrete, wood, and other materials [1]. However, traditional manufacturing techniques, which often limit the design flexibility of cemented carbides, suggest that additive manufacturing (AM) could present a promising alternative for the future processing of these materials [2–4].

AM has signified a pivotal shift in manufacturing paradigms, offering unprecedented flexibility in both the quantity and design of manufactured parts. It has facilitated the efficient production of bespoke tools and enabled mass customization and production on a large scale. This technology has unlocked the creation of a diverse array of products with intricate geometries, thereby enhancing functionality across various industries. AM has enabled innovative designs, such as optimized cutting geometries, chip chutes of various profiles and shapes, integrated cooling systems, and an increased number of cutting edges [5–7]. The fabrication of cemented carbide modules with integrated fluid channels or ports, which is challenging with traditional methods, has been simplified through AM [8–10]. Moreover, the production of cemented carbide nozzles using traditional methods is fraught with difficulties and high costs, and it is inherently restricted in terms of design optimization. In contrast, 3D printing technology has facilitated the efficient manufacturing of nozzles with complex features, such as curved channels, threads, and diverse mounting solutions, consequently reducing lead times [11]. Despite considerable research efforts dedicated to the development of AM processes for cemented carbides, no single AM technique has yet emerged as the dominant method for large-scale applications. The primary obstacle to this research and development conundrum stems from the absence of targeted investigations into the densification and microstructure evolution mechanisms that are specific to the unique attributes of the AM processing of carbides. Furthermore, the interconnections between these mechanisms and the design of feedstock carbide materials, the printing/sintering process, and the resulting mechanical behavior have not been adequately explored.

To date, the realm of additive manufacturing (AM) for the production of cemented carbides has been dominated by two principal methodologies, each with its own set of advantages and disadvantages. As shown in Table 1, the first methodology encompasses direct AM techniques, which integrate the processes of printing and sintering into a single, streamlined cycle. Prominent examples of direct AM include Selective Laser Melting (SLM) and Selective Electron Beam Melting (SEBM). The second methodology involves indirect AM techniques, which begin with the printing of an unfired green part, followed by traditional debinding and sintering processes to achieve the desired density of the cemented carbides. Techniques, such as Selective Laser Sintering (SLS), Binder Jetting (BJ), and 3D gel-printing (3DGP), are representative of this approach. The selection of the AM technique is crucial and must take into account the specific requirements and constraints of each application.

**Table 1.** Categories of AM techniques for cemented carbides.

Classifications	AM Techniques	Sections in This Paper	Pros and Cons
Direct AM	SLM	2.1, 4.1	Printing–sintering in one step, low efficiency and high cost, notable printing defects and decomposition of WC.

Table 1. Cont.

Classifications	AM Techniques	Sections in This Paper	Pros and Cons
Direct AM	SEBM	2.2, 4.2	Printing–sintering in one step, high efficiency, high cost, notable printing defects and decomposition of WC.
	SLS	2.3, 4.3	High printing efficiency, low cost, low relative density and mechanical properties.
Indirect AM	BJ	2.4, 4.4	High fabrication efficiency, low cost, high relative density and mechanical properties, low microstructure homogeneity.
	3DGP	2.5, 4.5	High sintering performance, high relative density, low dimensional accuracy, low fabrication efficiency.

## 2. Advanced Additive Manufacturing Techniques for Cemented Carbides

### 2.1. Selective Laser Melting (SLM)

Selective Laser Melting (SLM), also called Laser Powder Bed Fusion (LPBF), is a direct AM technique that utilizes a high-energy laser beam to selectively melt metal powders according to the layer-by-layer slice information derived from a three-dimensional model of the intended part [12]. As shown in Figure 1, the laser beam traces a precise path, melting the powder completely and fusing it under thermal influence. As the melted material cools and solidifies, it forms a solid layer, which is sequentially stacked upon with additional layers of powder until the complete model is constructed.

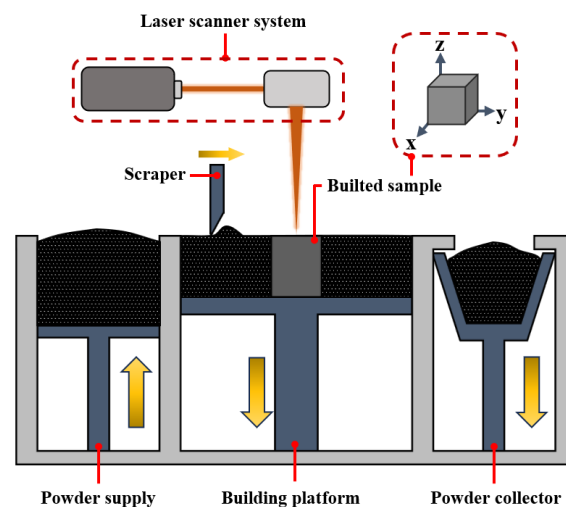


Figure 1. Schematic diagram of Selective Laser Melting (SLM) or Laser Powder Bed Fusion (LPBF).

Recent studies have highlighted the impact of the powder morphology on the SLM process. Chen et al. [13] reported that spherical WC-Co granules, as opposed to irregularly shaped granules, resulted in higher relative densities for WC-Co samples. However, the SLM process could lead to inhomogeneous microstructures and the rapid grain growth of WC [14], attributed to the non-uniform temperature distribution and varying dwell times in the liquid phase. A comparative analysis of hot-pressed and SLM-processed WC-20Co carbides revealed that both carbides exhibited a Vickers hardness surpassing 10 GPa, with the SLM-processed carbides showing a slightly lower hardness due to its lower density and coarser WC grains.

Grigoriev et al. [15] explored the SLM processing of WC-6Co with ultrafine Co particles, implementing a multidirectional scanning strategy to counteract anisotropy's effects on the

mechanical properties. The resulting samples achieved a hardness of HV2500, which was 1.6 times greater than that of the conventional materials. An X-ray diffraction (XRD) analysis indicated the presence of the carbon-deficient phase  $W_2C$  in the printed samples. In practice, the sintering temperature during the SLM process can exceed  $2000\text{ }^\circ\text{C}$ , significantly higher than the melting/sintering temperature of the WC-Co system ( $1300\text{ }^\circ\text{C}/1400\text{--}1480\text{ }^\circ\text{C}$ ). Meanwhile, the liquid-phase sintering time during the SLM process is as brief as  $10^{-3}\text{ s}$ , which is considerably shorter than the sintering time for traditional powder metallurgy processes (1–2 h). Consequently, achieving equilibrium sintering conditions during the SLM process is extremely challenging, making abnormal WC grain growth and even the decomposition of WC grains quite prevalent [16].

Liu et al. [16] conducted a comprehensive investigation into the microstructure and WC grain growth of WC-Co during the SLM process, supported by a finite element simulation. Their findings revealed that the microstructure and mechanical properties of the printed samples with varying Co content displayed anisotropy, with the relative density of the WC-Co samples increasing as the Co content increased. The maximum sintering temperature was determined by the interplay of the laser power and scanning speed. Figure 2 presents the typical microstructures of carbides processed via Selective Laser Melting (SLM). A carbon-deficient phase is commonly observed in these carbides. However, the inhomogeneity in the sintering temperature caused by the laser beam often leads to frequent occurrences of abnormal WC grain growth.

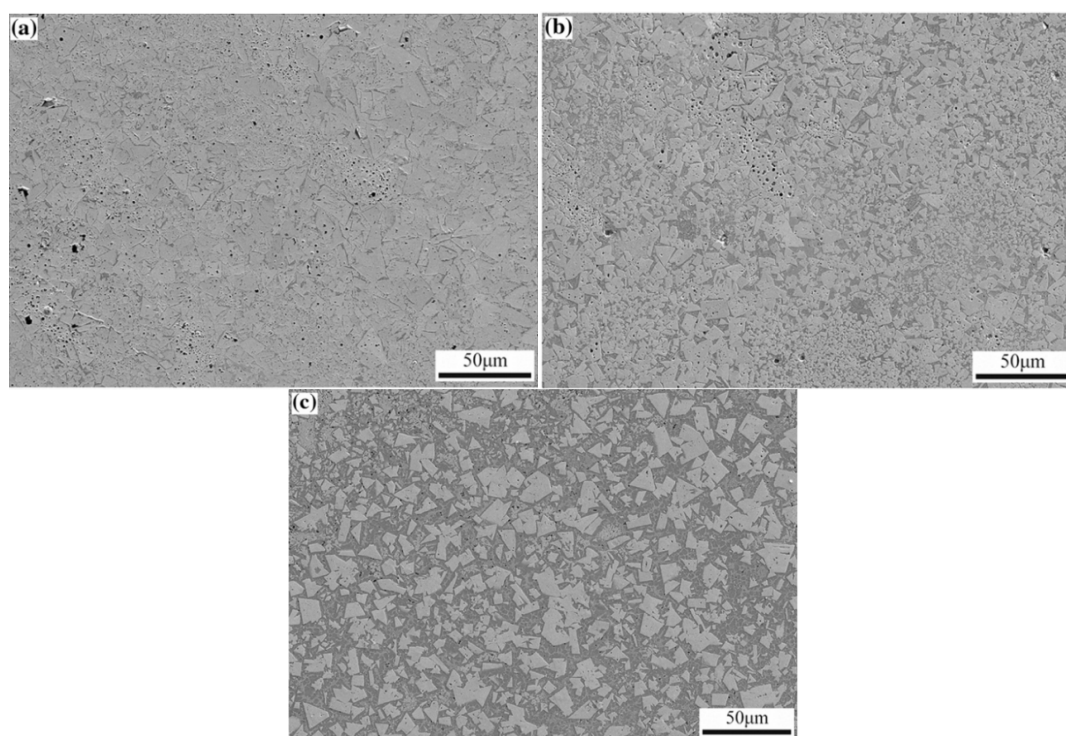


**Figure 2.** Microstructures of SLM-processed cemented carbides, showcasing the variability in the decomposition of WC and abnormal WC grain growth across the different compositions: (a) WC-12Co, (b) WC-20Co, and (c) WC-32Co [16].

A study on nano-structured WC-Co hardmetal containing 25 wt.% WC and 75 wt.% Co demonstrated remarkable resistance to thermal shocks during the SLM process [17]. The tungsten carbide particles were found to be homogeneously dispersed within the Co matrix, with no significant cracking observed. However, it was noted that an excessive Co content could compromise the alloy's strength and hardness. Increasing the scanning velocity was found to refine the microstructure and reduce the spheroidization effect.

It has been demonstrated that during the SLM process, a high relative density can be achieved through a high energy input, while a high cobalt content can be maintained with a low energy input [18]. A high laser energy density facilitates the formation of a coherent molten pool, resulting in high-density samples, but this also increases the brittleness of the cemented carbide. Meanwhile, a high Co content minimizes cracking formation and maximizes the density of the fabricated parts.

Li et al. [19] conducted a study on the effects of the SLM process on the microstructure and properties of a special cemented carbide system containing a high-entropy alloy binder (NiAl-CoCrCuFe). The hardness and toughness of the SLM-processed carbides revealed a clear gradient trend from the bottom (close to the baseplate region) to the upper portion. The Vickers hardness gradually increased from the region close to the baseplate to the upper portion. The baseplate region was characterized as having more metal binder, while the upper portion was mainly composed of a  $W_2C$ /metal dendritic matrix, with evenly distributed WC precipitates and h-carbide.

Xing et al. [20] successfully fabricated WC-12Co cemented carbides using the LPBF process. Their study examined the microstructural and mechanical property evolution of these carbides after post-sintering treatments. Figure 3a,b show significant thermal cracking and porosity in the as-fabricated WC-12Co carbides. Additionally, they observed WC phase decomposition and abnormal grain growth, which can impair the material's mechanical integrity. The post-sintering process, detailed in Figure 3c–f, significantly altered the microstructure, reducing thermal cracking and porosity, and enhancing the material density and homogeneity. Low-carbon phases, such as  $W_2C$  and  $Co_3W_3C$ , which can compromise performance, were notably reduced due to the carbon compensation during post-sintering, as shown in Figure 4. This figure illustrates the effective redistribution of carbon within the microstructure, stabilizing the WC phase and mitigating phase decomposition. The post-sintering process profoundly improved the mechanical properties of the LPBF-processed WC-12Co carbides, increasing the compressive strength by over 300% compared to the as-LPBF-processed material. This enhancement was attributed to the elimination of defects, the refinement of grain boundaries, and the optimization of the phase distribution. Xing et al.'s findings highlight the critical role of post-sintering in the LPBF processing of carbides, not only correcting microstructural anomalies but also significantly enhancing the final product's mechanical properties.

The incorporation of nickel is widely recognized for its ability to enhance the wear resistance of cemented carbides. Gu et al. [21] successfully synthesized WC-Ni cemented carbide through a specialized in situ reaction within a W-Ni-C system, utilizing the Selective Laser Melting (SLM) process. During their investigation, Gu et al. observed that the SLM process parameters, particularly the scanning speed, had a profound impact on the microstructure and, consequently, the performance of the WC-Ni cemented carbides. They noted that excessively high scanning speeds can result in the formation of cavities and cracks within the material, as well as the significant growth of WC grains, which can compromise the material's integrity and performance. To optimize the SLM molding process for WC-Ni composite powder, Ergüder et al. [22] employed a meticulous feedstock carbide powder design. The process began with the uniform coating of a 400 nm nickel layer on WC powder through the technique of electroless plating. This step was crucial for ensuring the homogeneous distribution of the nickel. Following this, the researchers determined the optimal process parameters for the SLM method using the Ni-coated WC powder. These parameters were critical for achieving a high relative density close to 99%. The resulting material exhibited a hardness value of 1962 HV, highlighting the superior mechanical properties achieved through this process. Furthermore, wear testing was conducted to evaluate the influence of the hatch spacing on the wear resistance of the SLM

carbides. Their findings, as depicted in Figure 5, demonstrate that the hatch spacing is a critical parameter affecting the wear resistance of the material. Specifically, a 60% hatch spacing was found to yield the lowest coefficient of friction, the lowest wear rate, and the highest microhardness among the tested specimens.

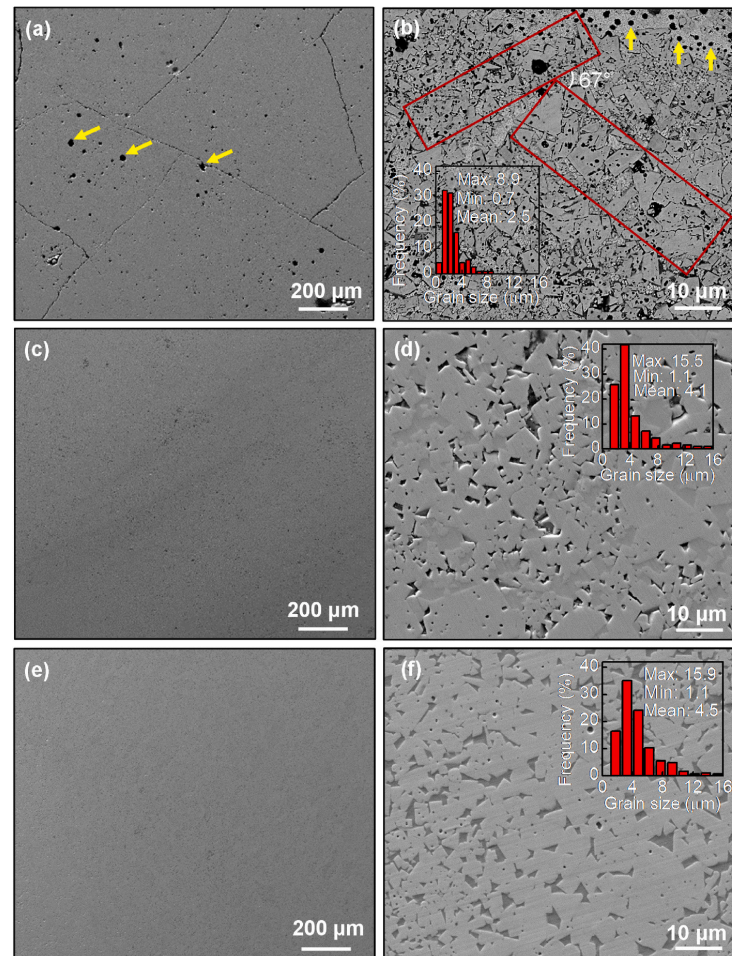


**Figure 3.** Typical microstructure of LPBF-processed WC-12Co carbides (a,b) without and (c–f) with post-sintering, (c,d) through post-sintering at 1390 °C, and (e,f) through post-sintering at 1480 °C [20]. Post-sintering significantly reduces cracking and improves the microstructure quality.

The fabrication of cemented carbides through the SLM process frequently results in the presence of numerous cracks and warpings. In addition, abnormal WC grain growth, the decomposition of the WC, and the formation of an h-phase have been widely documented [13–16,20]. These defects are predominantly due to the extremely high local sintering temperature and non-uniform thermal distribution that occurs during the SLM procedure. The localized melting of the powder particles creates a molten pool, which, when contrasted with the cooler surrounding material, establishes a significant temperature gradient. This disparity in temperature leads to the generation of considerable longitudinal and transverse tensile residual stresses within the material after the solidification phase. These residual stresses can act as initiation sites for cracks and contribute to the warping of the final product, thereby impacting the structural integrity and mechanical performance of WC-Co carbides.

Furthermore, the elevated temperatures characteristic of the SLM process can induce the evaporation of cobalt (Co), a key component that enhances the toughness of the WC-Co material. The loss of Co from the material can result in a reduction in its fracture toughness, making it more susceptible to brittle failure under stress. This decrease in toughness is

a critical concern, as it directly affects the material’s ability to withstand the demanding conditions encountered in various industrial applications, such as cutting tools and wear-resistant components. The current research status of the SLM process for cemented carbides is listed in Table 2.

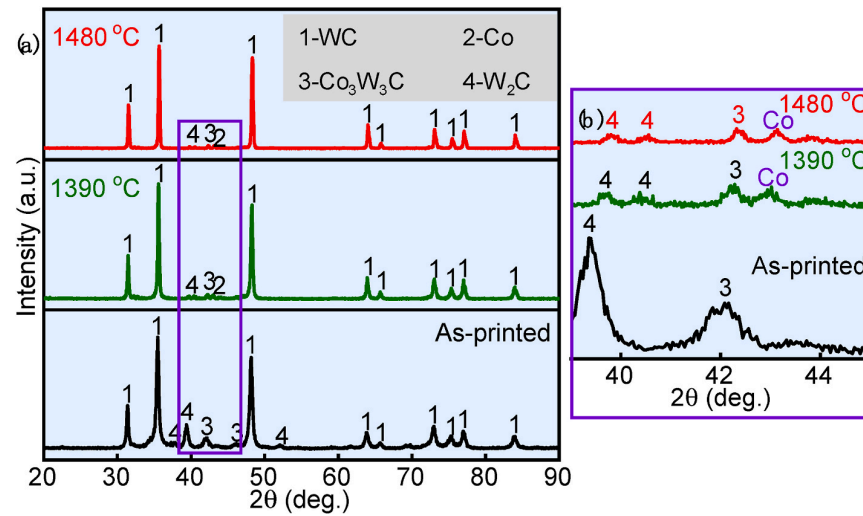


**Figure 4.** (a) XRD patterns of LPBF-processed WC-12Co carbides with and without (“As-printed”) post-sintering at 1390 °C and 1480 °C; (b) the magnified view of the diffraction peaks in the 2θ range of 39–45° (purple frame in (a)) [20]. The XRD patterns confirm that the post-sintering notably reduces the low-carbon phases.

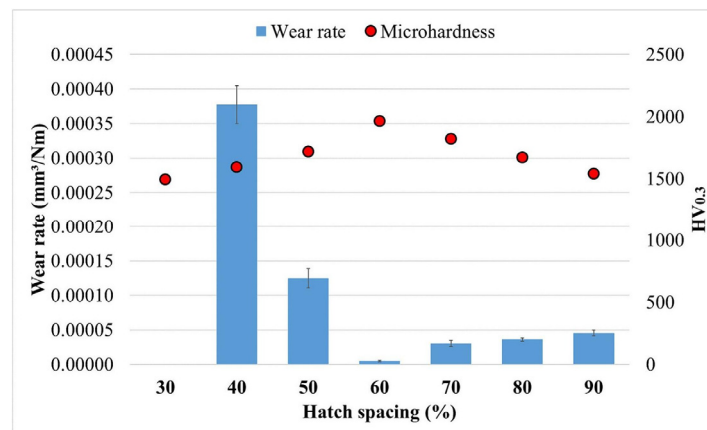


**Figure 5.** Wear rates and microhardness of SLM-processed carbides as a function of the hatch spacing [22]. The optimum hatch spacing substantially improves both the microhardness and wear resistance.

**Table 2.** Current research status of SLM process for cemented carbides.

Representative References	Materials	Key Studied Parameters	Key Findings
[13]	WC-20Co	Effect of the morphology of feedstock carbide granules, anisotropic microstructure	<ol style="list-style-type: none"> <li>Spherical-shaped carbide granules, as compared with irregular-shaped ones, significantly enhance printing performance.</li> <li>SLM often introduces abnormal WC grain growth, leading to anisotropic lamellar microstructures.</li> </ol>
[14]	WC-12Co	Types of feedstock carbide granules (micron vs. nano WC), microstructure	Significant and inhomogeneous WC grain growth, as well as decarburization of WC and the formation of low-carbon phases, are commonly observed in SLM-processed carbides.

Table 2. Cont.

Representative References	Materials	Key Studied Parameters	Key Findings
[15]	WC-6Co	Feedstock carbide powder preparation, mechanical property comparison between SLM and conventional processes	SLM induces significant thermal cracking. However, carbides processed via SLM exhibit higher hardness and wear resistance compared to those processed using conventional methods.
[16]	WC-12Co, WC-20Co, and WC-32Co	Effect of Co content, microstructure evolution and WC grain growth mechanisms, simulation of SLM process	<ol style="list-style-type: none"> <li>1. Higher Co content in feedstock carbide powders suppresses WC grain growth during the SLM process.</li> <li>2. The primary mechanisms of WC grain growth during SLM include dissolution–deposition and agglomeration, with the latter being more pronounced in low-Co carbides.</li> <li>3. The SLM process induces significant anisotropy in both the microstructure and mechanical properties.</li> </ol>
[17]	WC-75Co	Feedstock carbide powder with nano WC	A higher Co content helps to mitigate thermal cracking. SLM achieves extremely high cooling rates, reaching up to $10^6$ K/s.
[18]	WC-12Co, WC-17Co	Effect of SLM parameters on relative density and Co content of carbides	The energy density of the SLM process has a double-edged effect. While higher energy density enhances relative density, it also leads to more significant cobalt evaporation.
[19]	Cast Carbide-20NiAlCoCrCuFe high-entropy alloy	The dilution effect of baseplate	The dilution effect from the baseplate and elemental evaporation during the SLM process contribute to the formation of gradient microstructures and hardness profiles in carbides.
[20]	WC-12Co	Microstructure, post-sintering, cutting performance	Post-sintering significantly reduces the cracking and low-carbon phases introduced by SLM, thereby improving microstructure quality and mechanical properties.
[21]	85W-5C-10Ni	In situ WC formation, metallurgical mechanisms	<ol style="list-style-type: none"> <li>1. In situ WC/Ni<sub>2</sub>W<sub>4</sub>C cemented carbides were fabricated using SLM from a W–Ni–graphite powder mixture. A relative density of 96.3% was achieved at high laser energy input.</li> <li>2. The WC phase developed through multi-laminated growth mode, with its morphology evolving from block-shaped to triangular to elliptical as the applied linear energy density decreased.</li> </ol>
[22]	Ni-coated WC powder	Electroless Ni-plating process, SLM parameters, friction and wear testing	<ol style="list-style-type: none"> <li>1. Ni plating on WC powder is essential for achieving a relative density of 99%.</li> <li>2. The microstructure exhibits a dendritic structure with some cracking.</li> <li>3. Optimizing the hatch spacing significantly enhances both microhardness and wear resistance.</li> </ol>

## 2.2. Selective Electron Beam Melting

Selective Electron Beam Melting (SEBM) has emerged as an apt additive manufacturing technique, particularly well suited for the fabrication of alloys that possess high melting points or are prone to oxidation and nitrogen absorption [7]. This process shares similarities with SLM in its fundamental approach of a layer-by-layer deposition of metal powder onto a metal substrate. However, SEBM distinguishes itself by employing a high-energy electron beam, rather than a laser, to melt the powder within a vacuum environment, as illustrated in Figure 6. This environment is critical for preventing oxidation and ensuring the purity of the melted material.

The SEBM process allows for a higher substrate preheating temperature compared to SLM, which is essential for managing the thermal dynamics of materials with high melting points. This elevated temperature facilitates the melting process and can lead to an improved densification of the final product. Moreover, the scanning rate in SEBM is a pivotal parameter that significantly influences the quality of the manufactured parts [23]. The rate at which the electron beam scans across the substrate directly affects the melting

pool's temperature distribution, the coalescence of adjacent powder layers and, ultimately, the microstructure and mechanical properties of the consolidated parts.

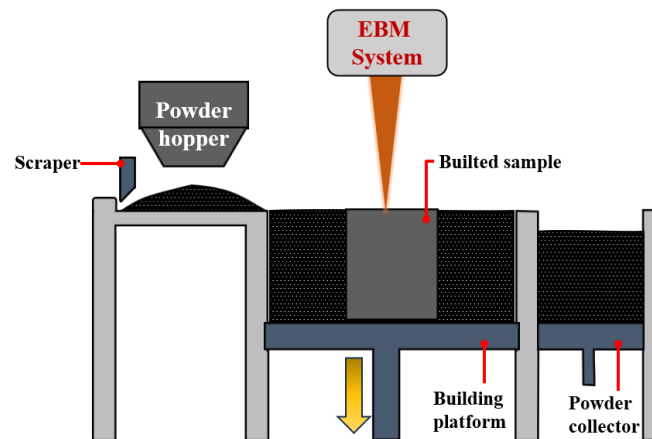


**Figure 6.** Schematic diagram of Selective Electron Beam Melting (SEBM).

The careful control of the scanning rate is therefore essential to optimize the SEBM process, ensuring the production of components with the desired geometric accuracy, surface finish, and mechanical integrity. By fine-tuning the process parameters, SEBM can be effectively utilized to manufacture complex components from high-performance alloys that are otherwise challenging to process using conventional methods. This makes SEBM an invaluable technique in the realm of advanced materials science and engineering, particularly for applications in aerospace, automotive, and tooling industries, where high-strength and high-temperature resistance are paramount.

The concentration of cobalt (Co) in carbides synthesized via SEBM has been observed to be significantly influenced by the specific manufacturing conditions, leading to substantial deviations from the initial Co content present in the feedstock carbide powder. This variation suggests that a considerable amount of liquid Co evaporates during the additive manufacturing process, which could potentially alter the mechanical properties of the final product. It has been hypothesized that the high strains present among the tungsten carbide (WC) layers originate from the extremely high WC grain growth rates, particularly in layers containing abnormally large WC grains [7]. These strains are anticipated to have a substantial impact on the fracture toughness of carbide samples produced through SEBM.

Peng et al. [24] detailed the fabrication of cemented carbides with WC dispersed in a NiBSi matrix using the SEBM technique under a variety of fabrication conditions. Konyashin [25] utilized Selective Electron Beam Melting to shape WC-13Co samples, a process that resulted in the evaporation of some liquid Co and intense local WC grain growth. This led to the formation of unique microstructures in the cemented carbide particles, characterized by layers with medium-coarse and abnormally large WC grains. The near-surface layer of these cemented carbide particles exhibited high roughness, comparable to the mean size of the original WC-Co granules.

Wang et al. [26] prepared WC-12Co cemented carbides via SEBM, followed by a post-sintering heat treatment at 1400 °C and 5 MPa of argon pressure. As depicted in Figure 7, similar to carbides processed with SLM/LPBF, anisotropic microstructures are evident in SEBM-processed carbides.

The observation of alternative layers of coarse and fine WC grains in Figure 7 is attributed mainly to the inhomogeneous liquid-phase sintering, and the  $\eta$  phase is commonly present in WC-12Co cemented carbide, resulting from the partial decomposition of WC and its reaction with Co. The post-sintering heat treatment reduces the anisotropy of the microstructure and the  $\eta$  phase to a certain extent, but does not completely eliminate them.

The friction and wear testing results, as shown in Figure 8, indicate that the post-sintering heat treatment increased both the friction coefficient and wear rate of the SEBM-processed carbides, primarily due to the substantial WC grain growth. These findings underscore the importance of optimizing post-processing treatments to mitigate the effects of grain growth and enhance the tribological properties of SEBM-manufactured carbides.

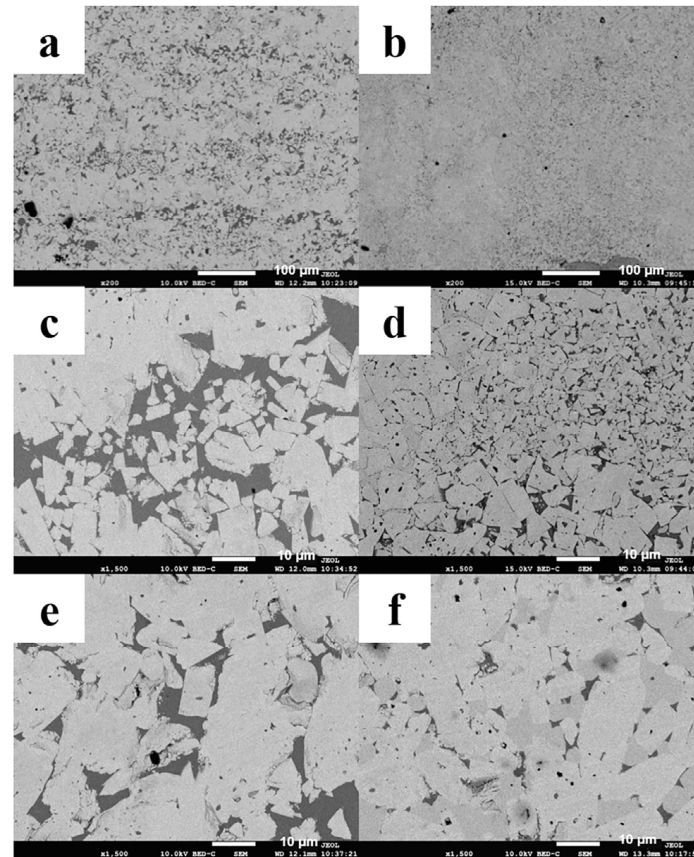


**Figure 7.** Microstructure of (a,c,e) longitudinal sections and (b,d,f) cross sections of (a–d) SEBM-processed WC-12Co carbides, and (e,f) post-sintering-treated specimens [26]. SEBM process introduces apparent microstructure inhomogeneity, which can be mitigated via post-sintering treatment.

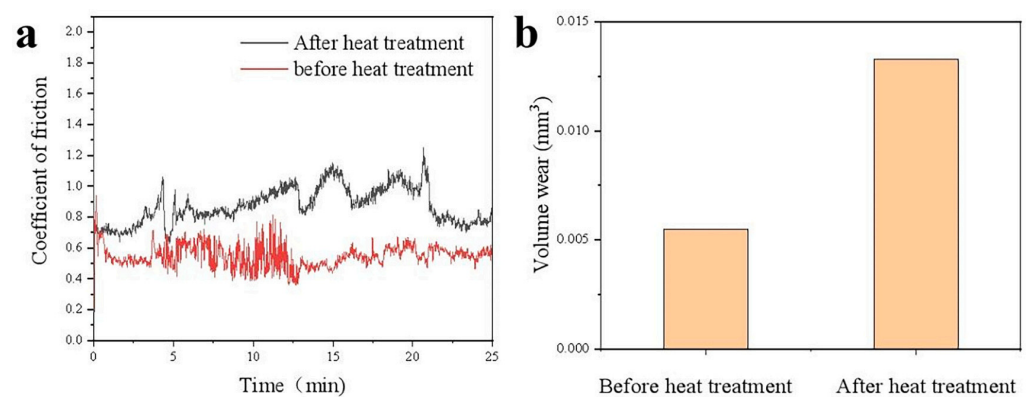


**Figure 8.** (a) Friction coefficients and (b) wear rate of SEBM-processed WC-12Co carbides before and after post-sintering heat treatment [26]. Post-sintering increases the COF and reduces the wear resistance of SEBM-processed carbides.

The current research status of the SEBM process for cemented carbides is listed in Table 3.

**Table 3.** Current research status of SEBM process for cemented carbides.

Representative References	Materials	Key Studied Parameters	Key Findings
[24]	Cast Carbide-35NiBSi	Feasibility of SEBM, microstructure and mechanical properties	1. During the SEBM process, interfacial dissolution of the cast carbide and inter-diffusion of elements between the matrix and the cast carbide were observed.
[25]	WC-13Co	Feedstock carbide granule preparation, microstructure analysis, printing parameters, post-sintering	1. SEBM can produce fully dense carbides without a post-sinter-hip process; however, the post-sinter-hip process does enhance both density and microstructure quality. 2. Co evaporation and abnormal WC grain growth, leading to a layered microstructure, are commonly observed in SEBM-processed carbides. 3. SEBM results in high surface roughness of carbides.
[26]	WC-12Co	Microstructure, mechanical properties, post-sintering	1. In carbides processed by SEBM, an anisotropic microstructure is observed, characterized by abnormal WC grain growth that results in the layered microstructure of the longitudinal section, as well as the formation of low-carbon phases. 2. While post-sintering can mitigate microstructural inhomogeneity to some extent, it also reduces the wear resistance of SEBM-processed carbides.

### 2.3. Selective Laser Sintering

Selective Laser Melting (SLM) and Selective Laser Sintering (SLS) are two discrete AM processes that, despite occasional conflation, are fundamentally different in their operational mechanisms. The principal distinction between SLM and SLS lies in the extent of melting involved: SLS, essentially an indirect AM process, involves the bonding of feedstock powder mainly through the use of organic binders for the melting process, while SLM entails partial or complete melting of the feedstock powder rather than any organic binders. Post-processing for SLS is essential, as it requires debinding and sintering or infiltration to achieve the desired high-density characteristics [27–31].

Kumar et al. [28,29] conducted an in-depth investigation into the SLS processing of a range of carbides, including WC-18Cu-12Co, WC-9Co, WC-12Co, WC-17Co, and WC-50Co. Their comprehensive approach included the carbide design, SLS process optimization, and infiltration, all aimed at overcoming the inherent limitations of the SLS technique. The researchers applied a bronze infiltration to the SLS-processed carbides to achieve final densification, concluding that this method significantly bolstered the mechanical and wear properties of AM-produced cemented carbides without compromising the product's dimensional integrity. Moreover, their work evidenced a marked enhancement in the wear resistance of post-processed SLS cemented carbides.

In another study by Jucan et al. [30], WC-Co/PA12 specimens with 15% and 20% PA12 by weight were successfully fabricated using the SLS technique. These specimens achieved a relative density of 65% after undergoing a subsequent sinter-hip process at 1400 °C and 50 bar of argon pressure. The typical microstructure of these specimens is depicted in Figure 9. This study underscores the importance of utilizing WC-Co powders with a higher bulk density and/or increasing the cobalt content to attain high densification of the samples.

Furthermore, Gâdâlean et al. [31] fabricated WC-10Co and WC-12Co carbides through the SLS process, utilizing high-bulk-density powders. Following a sinter-hip process at 1400 °C with 50 bar of argon pressure, these carbides reached a maximum relative density of over 80%. This achievement underscores the potential of SLS for producing high-density carbide components when high-bulk-density powders are employed.

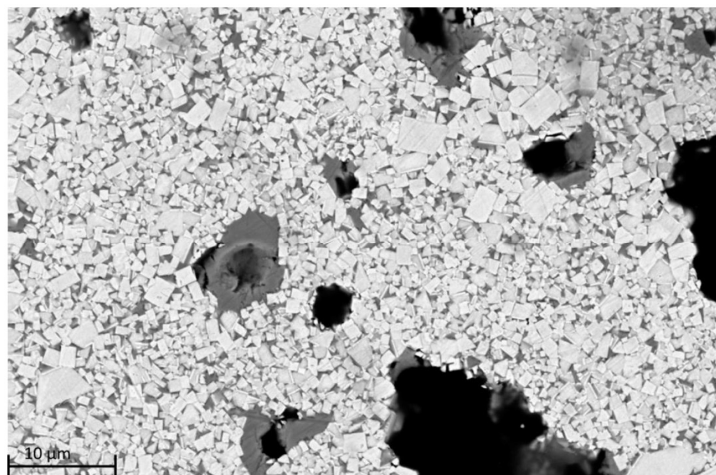


**Figure 9.** Microstructure of SLS-processed WC-12Co carbide after sinter-hip treatment [30]. Apparent porosity exists after sintering, indicating the significant challenge of SLS processing of carbides.

The current research status of the SLS process for cemented carbides is listed in Table 4.

**Table 4.** Current research status of SLS process for cemented carbides.

Representative References	Materials	Key Studied Parameters	Key Findings
[28,29]	WC-9Co, WC-12Co, WC-17Co, WC-18Cu-12Co, and WC-50Co, bronze infiltration	Feedstock materials, SLS process parameters, infiltration process	<ol style="list-style-type: none"> <li>1. The SLS process, when combined with bronze infiltration, can yield high-density carbides.</li> <li>2. Optimizing SLS process parameters is essential for achieving this high density.</li> </ol>
[30,31]	WC-10Co, WC-12Co	Sacrificial binder polyamide (PA12) content, feedstock powder preparation, effect of carbide granule density, sinter-hip process	<ol style="list-style-type: none"> <li>1. Directly mixing carbide granules with coarse sacrificial binder powder is viable for the SLS process, although the relative density remains low after sinter-hip processing.</li> <li>2. Increasing the density of carbide granules can enhance the final sintered density of carbides processed via SLS.</li> </ol>

#### 2.4. Binder Jetting Additive Manufacturing

Binder Jetting Additive Manufacturing (BJAM), also known as BJ3DP, is a widely adopted 3D printing technology that caters to a diverse range of materials, including metals, ceramics, and polymers. BJAM is a cost-effective process that generally involves several stages [32]. This innovative process initiates with the meticulous deposition of a powder layer onto a powder bed, as illustrated in Figure 10. Following this, an adhesive is precisely sprayed onto the designated printing area of the layer through an array of micro-nozzles, which serves to bind the powder particles together. The adhesive-bound layer is then subjected to heating and drying. Then, the process of powder spreading combined with binder spraying, heating, and drying is iteratively repeated until the entire structure is meticulously constructed [33]. Once the printing is complete, the sample is

exposed to a controlled thermal environment for curing, debinding, and sintering. This post-processing step is critical for achieving full density and enhancing the mechanical properties of the part, ensuring its structural integrity and performance.

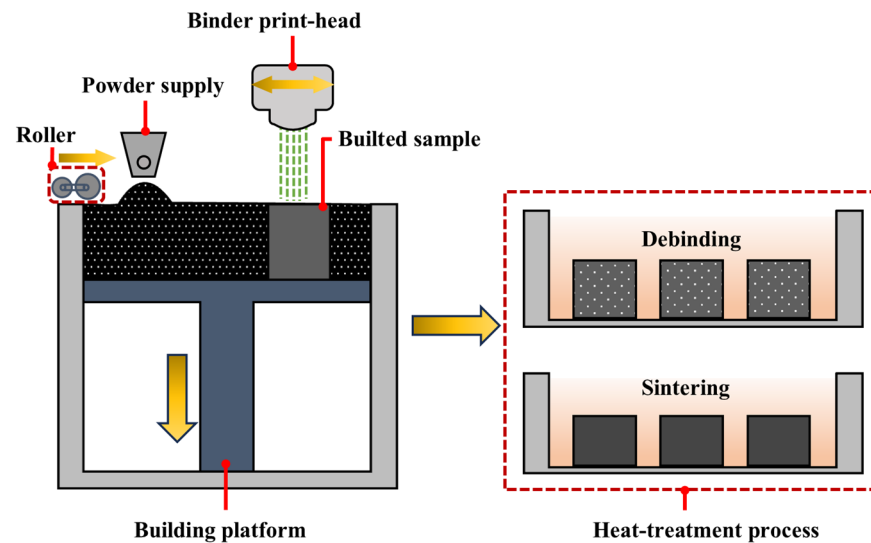


**Figure 10.** Schematic diagram of Binder Jetting Additive Manufacturing (BJAM).

In contrast to high-energy beam-based 3D printing technologies, such as Selective Laser Melting (SLM) and Selective Electron Beam Melting (SEBM), BJAM offers a suite of unique benefits. These include reduced costs, a broader range of material systems, superior surface quality, and the elimination of the need for support structures, which can be a significant advantage in terms of both material conservation and post-processing efficiency.

The printing parameters in BJAM, such as binder saturation, binder set time, drying time, and layer thickness, significantly influence the properties of the printed blanks and the final sintered parts. These parameters must be meticulously optimized to achieve the desired material characteristics and dimensional accuracy. The binder saturation level, in particular, plays a crucial role in determining a part's green strength, while the drying time and layer thickness directly affect a part's dimensional stability and surface finish. Therefore, a comprehensive understanding of these parameters is essential for harnessing the full potential of BJAM for the production of high-quality 3D-printed components.

In their seminal work, Enneti et al. [34] conducted a thorough investigation into the effects of the binder saturation and powder layer thickness on the green strength of WC-12Co printed samples. Their study meticulously detailed the phenomena of binder infiltration and spreading that occur when a binder droplet interacts with a powder layer. The research revealed that the powder layer thickness and binder saturation are two independent parameters, and at a constant powder layer thickness, the green strength of the carbide samples increased with higher binder saturation levels. This enhancement in strength was attributed to the binder's ability to more effectively penetrate and disperse within the powder layer, thereby enhancing the mechanical interlock between the particles. Furthermore, the study demonstrated that the carbide samples printed with a 14 s binder set time exhibited superior strength compared to those printed with a 7 s set time. This increase in strength was attributed to the extended period, allowing for a more comprehensive binder infiltration and spreading within the powder layer, leading to a more robust green body. However, when the powder layer thickness was substantially increased to achieve a 75% binder saturation, a notable decrease in the sample strength was observed. This decline in strength was attributed to the binder's limited spreading capability at higher thicknesses, as the majority of the binder was consumed by the infiltration process, leaving an insufficient binder to spread across the powder layer's surface and form a cohesive

bond. The findings underscore the critical interplay between the binder saturation, powder layer thickness, and the resulting green strength of the printed components. These insights are crucial for optimizing the Binder Jetting process to achieve the desired balance between green strength and part geometry, which ultimately influences a sintered part's mechanical properties and dimensional accuracy.

Upon the completion of the BJAM printing phase, the subsequent steps of curing, debinding, and sintering are imperative for the enhancement of the mechanical properties of cemented carbide prints. In their pivotal study, Mostafaei et al. [35] determined that the relative densities of BJAM-processed WC-12.5Co carbide can attain values between 97 and 100% following a sinter-hip procedure at a temperature of 1435 °C and an argon pressure of 6.1 MPa. This finding underscores that the combination of Binder Jetting with a subsequent heat treatment is adept at yielding defect-free carbides with satisfactory properties from WC-Co composite powders. Furthermore, Mariani et al. [36] scrutinized the impact of the printing parameters and the sintering process on the mechanical properties of BJAM-derived WC-12Co. They observed that the relative densities of samples sintered in a vacuum and under pressure (35 bar) were 97.4% and 99.3%, respectively. Pressure sintering was particularly effective at obliterating closed pores within the samples, thereby enhancing their density and mechanical integrity. Kumar et al.'s investigation [37] revealed that non-spherical feedstock carbide powder was more prone to achieving higher sintered densities compared to spherical feedstock powder, owing to the higher capillary pressure that facilitates more efficient densification. Enneti et al. [38] substantiated the capability of BJAM and sinter-hip processes for manufacturing WC-Co parts with desirable mechanical properties. The printed WC-12Co samples achieved full density after sintering under 1.83 MPa pressure at 1485 °C. The hardness and fracture toughness of these fully sintered samples were found to be on par with those of conventionally produced WC-12Co with a medium WC grain size. During the debinding and sintering phases, the shrinkage of the samples was within the range anticipated for powder injection molding and extrusion processes, which was approximately 20–25% in all three dimensions. This dimensional consistency is crucial for the precision and reliability of the final product. A microstructural examination of the BJ-processed carbide samples, as illustrated in Figure 11, reveals a degree of heterogeneity, with clusters of coarse WC grains interspersed among finer WC grains. This variation is attributed to the significant gap between the WC-Co granules during the BJ powder-spreading process, which promotes the abnormal grain growth of the WC, leading to the formation of coarse WC grain clusters or large Co pools. Such microstructural nuances have implications for the BJ-processed carbides' mechanical properties, including their wear resistance and fracture toughness, and are therefore of paramount importance in the optimization of the BJAM process for carbide manufacturing.

Enneti et al. [39] conducted an exhaustive evaluation of the wear performance of BJ-processed WC-12% Co cemented carbides, adhering to the stringent ASTM B611 [40] and G65 [41] test methods. Their findings revealed that the wear resistance of the WC-12Co material, fabricated through the BJAM process, notably exceeded that of standard cemented carbides, with a comparable cobalt content mainly due to the dual WC grain sizes of the BJ-processed carbides. This discovery underscores the potential of BJAM for producing wear-resistant materials that outperform their traditional counterparts. In a parallel study, Wolfe et al. [42,43] delved into the microstructure and mechanical behavior of BJAM-processed WC-10-17Co carbides, which spanned a range of WC grain sizes. Their study revealed that the use of coarse-grade WC resulted in the uniform distribution of WC grain sizes during the sintering process, which, in turn, contributed to an enhanced transverse rupture strength. In addition, their comprehensive investigation observed abnormal WC grain growth in both WC-12Co and WC-17Co carbides with medium WC particle

sizes [43], leading to the formation of a typical dual microstructure upon sintering treatment. This unique microstructural development is believed to contribute to the enhanced wear properties of these materials. As detailed in Table 5, a comprehensive summary of the wear-testing results for BJ-processed carbides is compiled. The wear resistance, assessed according to ASTM B611 [40] and G65 [41] standards, demonstrates that WC-12Co carbides with a dual microstructure (designated as WC720A12 and WC721A12) exhibit superior wear resistance compared to conventionally processed cemented carbides. This superiority is attributed to the optimized distribution of the WC grains. Conversely, the wear resistance of extra-coarse grades of WC-10Co and WC-12Co carbides (denoted as WC780A10 and WC780A12), which possess uniform microstructures, is found to be equivalent to that of conventional cemented carbides [43]. Although the formation of a typical dual microstructure, stemming from the abnormal WC grain growth during the sintering of BJ-processed carbides, may confer a certain level of enhanced wear resistance, the prevailing consensus in the academic and industrial communities is that the detrimental effects of abnormal WC grain growth on the mechanical behavior of carbides outweigh the benefits. This perspective is grounded in the understanding that abnormal WC grain growth can lead to microstructural inhomogeneities, which can compromise a material's overall performance. The negative impact of abnormal WC grain growth is multifaceted. It can result in a reduction in a material's fracture toughness due to the increased likelihood of grain boundary weaknesses and the potential for crack propagation along these boundaries. Additionally, large WC grains can create stress concentration points, making a material more susceptible to premature failure under a load. In summary, while the dual microstructure resulting from abnormal WC grain growth may provide some enhancement of wear resistance, the overall negative impact on the mechanical properties of BJ-processed carbides is a subject of significant concern. Continued research and development efforts are being directed towards mitigating these effects to harness the full potential of BJ-processed carbides in industrial applications where high-performance carbides are essential.

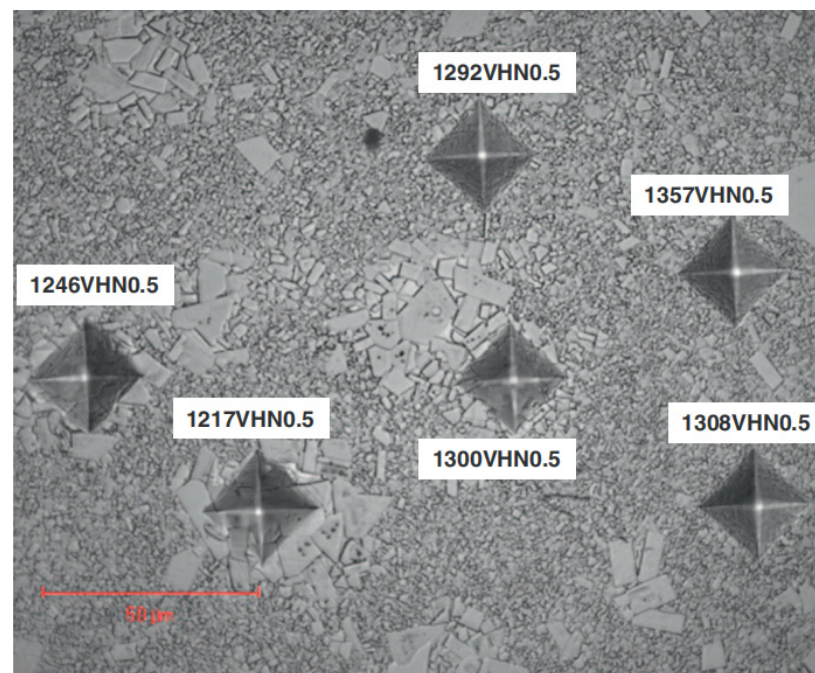


**Figure 11.** Heterogeneous microstructure and consequent uneven hardness distribution of BJAM-processed WC-12Co carbide [38]. Abnormal WC grain growth and clusters of coarse WC are easily observed for BJAM-processed carbides.

**Table 5.** Wear properties of BJ-processed WC-Co materials [43].

Powder Type	Chemical Composition	Initial WC Particle Size	B611 Volume Loss (mm <sup>3</sup> )	G65 Volume Loss (mm <sup>3</sup> )
WC720A12	WC-12%Co	Medium	140.5 ± 2.7	3.7 ± 0.7
WC721A12	WC-12%Co	Medium	113.5 ± 5.1	1.2 ± 0.1
WC780A10	WC-10%Co	Extra Coarse	239.3 ± 3.7	4.0 ± 0.2
WC780A12	WC-12%Co	Extra Coarse	282.2 ± 2.7	4.3 ± 0.2

One of the primary challenges associated with the BJ process for carbide production is the substantial shrinkage that occurs during the sintering treatment. This shrinkage significantly impacts the precision control of the dimensions and the geometric integrity of complex-shaped carbide components, potentially leading to deviations from the intended design specifications. To address this critical issue, Cramer et al. [44–46] implemented an infiltration approach for the production of BJ-processed cemented carbides, aiming to reduce post-sintering shrinkage. Their methodology involved the utilization of pure tungsten carbide (WC) powder to fabricate a green part through BJ printing. This green part was then subjected to a pressureless infiltration process with Co. The infiltration strategy employed by Cramer et al. demonstrated a remarkable reduction in shrinkage by approximately 15%, which was a significant advancement in the field. However, the infiltration process presents its own set of challenges, primarily concerning the precision control of the final Co binder content within the carbide matrix. Accurate control of the Co content is essential, as it directly influences a material's mechanical properties' consistency, including its hardness, toughness, and wear resistance. The current research status of the BJAM process for cemented carbides is presented in Table 6.

**Table 6.** Current research status of BJAM process for cemented carbides.

Representative References	Materials	Key Studied Parameters	Key Findings
[34,35]	WC-12Co, WC-12.5Co	Effect of binder saturation, powder layer thickness, and drying time	<ol style="list-style-type: none"> <li>Increasing binder saturation enhances the strength of green parts and reduces the strength disparity between samples printed with 60 and 70 μm powder layers, rather than extending the binder set time.</li> <li>A longer drying time is essential for improving the strength of green parts.</li> <li>Increased binder saturation may lead to the formation of Co-rich pools and h-phases.</li> </ol>
[36]	WC-12Co	Effect of WC grain size or phase status inside the feedstock carbide granules	<ol style="list-style-type: none"> <li>The presence of coarse WC in the feedstock carbide granules leads to coarse WC grain sizes post-sintering.</li> <li>W<sub>2</sub>C in the feedstock granules is eliminated during the sintering process.</li> </ol>
[37]	WC-10Co	Simulation of capillary force and capillary pressure during liquid-phase sintering of BJ-processed carbides, effect of feedstock powder morphology	Non-spherical feedstock carbide particles are more likely to achieve higher densification than spherical particles during liquid-phase sintering for BJAM-fabricated WC-10Co carbide, owing to the generation of higher capillary pressure.
[38,39]	WC-12Co	Sinter–HIP process, abnormal WC grain growth upon sintering	<ol style="list-style-type: none"> <li>The sinter–HIP process is essential for achieving high density in BJ-processed carbides.</li> <li>Abnormal WC grain growth is evident in BJ-processed carbides with a medium initial WC grain size, which is advantageous for enhancing wear resistance.</li> </ol>

Table 6. Cont.

Representative References	Materials	Key Studied Parameters	Key Findings
[42,43]	WC-10Co, WC-12Co, WC-17Co	Uniformity of WC grain size upon sintering, mechanical property comparison between BJ and conventional processes	<ol style="list-style-type: none"> <li>1. Coarse WC granules in the feedstock aid in producing uniform WC grain sizes after sintering of BJ-processed carbides, whereas medium WC sizes can induce abnormal WC grain growth during sintering.</li> <li>2. The mechanical properties of BJ-processed carbides are comparable to those of conventionally processed ones.</li> <li>3. BJ-processed carbides with a dual microstructure, characterized by abnormal WC grain growth, exhibit superior wear resistance compared to conventionally processed carbides.</li> </ol>
[44–46]	WC-19Co, WC-32–35 vol.% Co	Infiltration of BJ-processed carbides	Infiltrating BJ-processed pure WC with Co or Co-WC composites results in high density and minimal linear shrinkage.

### 2.5. Three-Dimensional Gel-Printing

Three-dimensional gel-printing (3DGP) represents a cutting-edge additive manufacturing technique that combines the principles of gel casting with those of Fused Deposition Modeling (FDM). This process, which has been variably termed as Powder Extrusion Printing (PEP) and Material Extrusion (MEX), among other nomenclatures, offers a unique approach to the fabrication of complex structures from metal or ceramic powders. As depicted in Figure 12, the 3DGP process is initiated by blending a metal or ceramic powder with an organic solvent, thereby creating a slurry or paste that serves as the printable material. During the printing phase, this slurry or paste is introduced into an extruder. The extrusion is facilitated by either compressed air or the mechanical rotation of a screw, which propels the material through a nozzle onto the printing platform. The nozzle is meticulously controlled to selectively deposit the slurry or paste in layers, thereby constructing the desired shape layer by layer. Following the extrusion, the organic components within the deposited slurry or paste undergo crosslinking and polymerization. This curing process solidifies the powder, resulting in the formation of a green part, which is the intermediate structure, before further processing. To complete the fabrication process, the subsequent steps of debonding and sintering are essential. These steps are aimed at eliminating the organic components and achieving the final densification of the metal or ceramic parts. Debonding involves the removal of the binder from the green part, a critical step that prepares the part for sintering. Sintering then follows, where the part is subjected to high temperatures to achieve the desired density and strength.

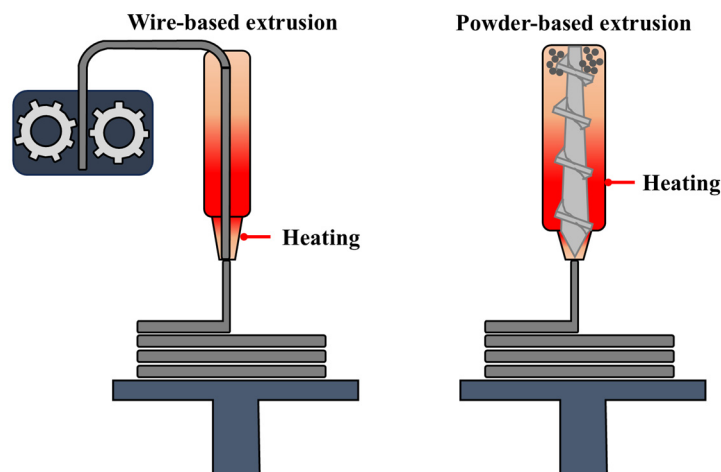
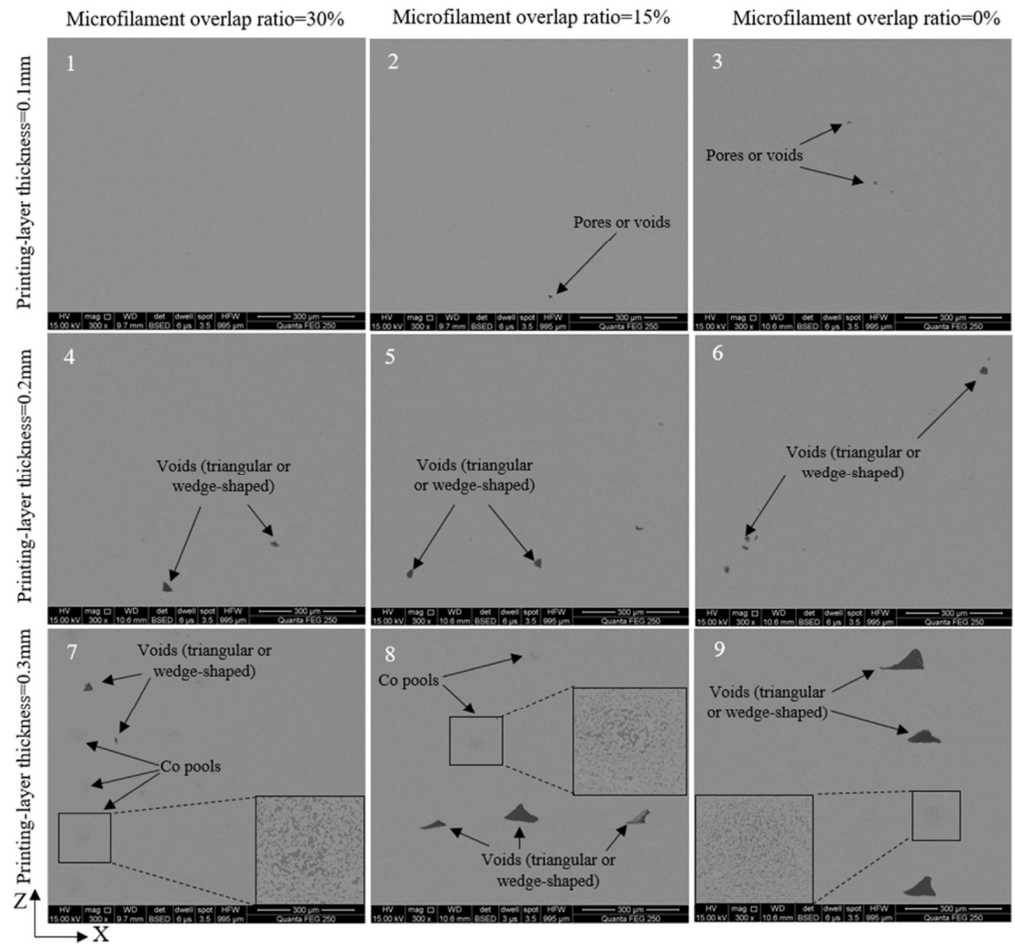


Figure 12. Schematic diagram of the extrusion and deposition system.

The 3DGP process, with its ability to handle a wide range of materials and its potential for high sintering performance, holds significant promise in the field of additive manufacturing. It presents a viable alternative for the production of the intricate parts and components that are required across various industries, from aerospace and automotive to biomedical applications. The versatility of 3DGP, coupled with its potential for customization and the ability to create parts with unique material properties, positions it as a formidable technique in the advancement of modern manufacturing.

Three-dimensional gel-printing has been instrumental in the fabrication of intricate carbide components, specifically the complex WC-20Co component referenced in [47]. The density and mechanical properties of the 3DGP-derived samples were significantly augmented by elevating the solid loading within the WC-20Co slurry. In a seminal study, Li et al. [48] adeptly prepared WC-8Co cemented carbide components employing the 3DGP process. They utilized a WC-8Co composite powder with an average particle size of 3.4 microns. The optimal concentrations of hydroxyethyl methacrylate (HEMA) and dispersant solspers-6000 were determined to be 1.71 wt% and 0.3 wt%, respectively, with a carbide powder content of 52 vol%. The resultant green body exhibited a strength of 25 MPa. Upon sintering at 1400 °C for a duration of 2 h, the relative density was 99%, with the hardness and transverse rupture strength of the samples measured at HRA90 and 2250 MPa, respectively. Chen et al. [49] fabricated WC-9Co carbide using the Material Extrusion (MEX) process, synonymous with 3DGP. Through meticulous feedstock powder design and optimization of the printing parameters, they successfully manufactured nearly fully dense carbides devoid of pores, cracks, or cobalt (Co) pools. The mechanical properties of the WC-9Co carbide were found to closely resemble those produced through traditional powder metallurgy processes. Figure 13 delineates the enhancement of the microstructure facilitated by the optimization of the printing parameters, including the printing layer thickness and microfilament overlap ratio.

In their seminal research, Zhao et al. [50] employed a paraffin/polymer binder composite as the principal raw material for the fabrication of WC-8Co carbide through the MEX process. Their investigation revealed that sintering under both a hydrogen and vacuum environment was pivotal for the efficient removal of residual carbon from the printed components. This process significantly contributed to the enhancement of the strength and hardness of the resulting products. Expanding upon these findings, Zhao et al. [51] subsequently refined the organic binder system, which comprised polyethylene glycol (PEG), polyvinyl butyral (PVB), high-density polyethylene (HDPE), and several other additives, for the preparation of MEX-processed WC-8Co carbides. Their research highlighted the critical role of polyvinyl butyral within the binder system, as it was instrumental in conferring strength to the green parts. A thorough comparative analysis of WC grain sizes, the final sintered density, and the mechanical properties of MEX-processed and traditional powder metallurgy-processed carbides across various sintering temperatures is delineated in Figure 14. This study demonstrates that the mechanical properties of MEX-processed carbides are closely comparable to those of carbides processed through traditional methods, albeit with a slight inferiority. This comprehensive analysis underscores the potential of the MEX process for producing carbides with mechanical properties that are nearly on par with those achieved through conventional powder metallurgy techniques, while also highlighting the importance of optimizing the binder system to achieve the optimal green part strength. Further research is warranted to bridge the slight gap in mechanical properties and to fully realize the potential of the MEX process for the manufacturing of high-performance carbides.



**Figure 13.** Microstructure improvement of WC-9Co carbide through 3DGP printing parameter optimization: printing layer thickness of (1–3) 0.1 mm, (4–6) 0.2 mm, and (7–9) 0.3 mm; microfilament overlap ratio of (1, 4, 7) 30%, (2, 5, 8) 15%, and (3, 6, 9) 0% [49]. Both the printing layer thickness and microfilament overlap ratio have critical effects on the final sintered density and microstructure quality of 3DGP-processed carbides.

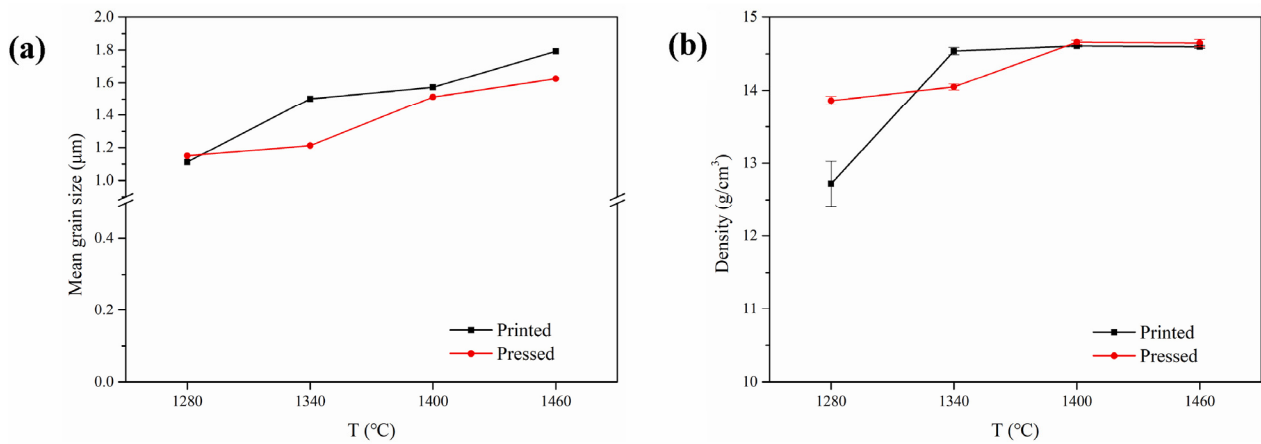


**Figure 14.** Cont.

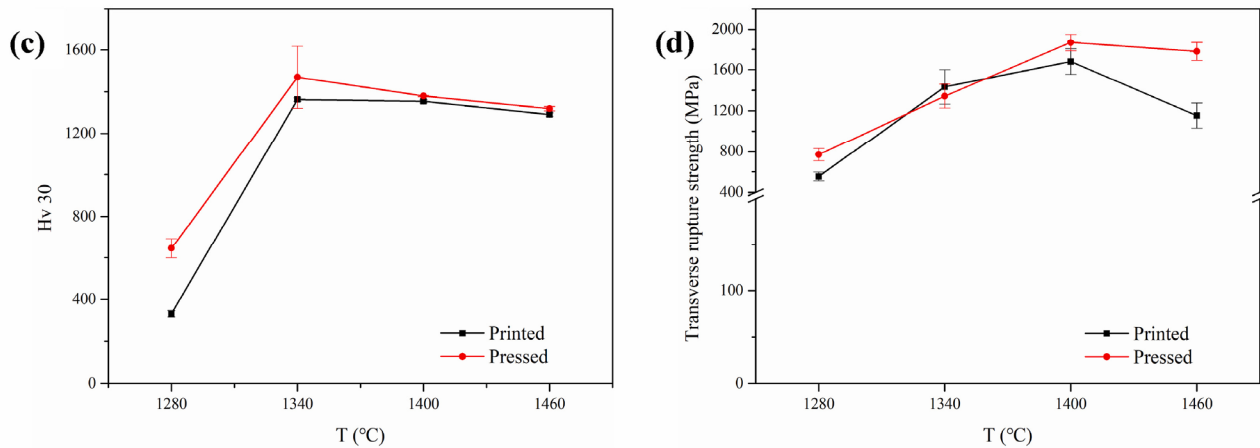


**Figure 14.** Microstructure and mechanical property comparison of MEX (3DGP)-processed (“Printed”) and traditional powder metallurgy-processed (“Pressed”) carbides: (a) WC grain size; (b) density; (c) hardness; and (d) transverse fracture strength [51]. Compared with traditionally processed carbides, 3DGP-processed carbides show slightly inferior mechanical properties.

The current research status of the 3DGP process for cemented carbides is listed in Table 7.

**Table 7.** Current research status of 3DGP process for cemented carbides.

Representative References	Materials	Key Studied Parameters	Key Findings
[47,48]	WC-8Co, WC-20Co	Gel system, solid loading, printing and sintering parameters	<ol style="list-style-type: none"> <li>Three-dimensional gel-printing is suitable for fabricating complex green bodies. Utilizing a fine nozzle enhances the forming accuracy of 3DGP and reduces the surface roughness of samples.</li> <li>Increasing the solid loading of WC-20Co slurry improves the slurry’s viscosity, green density, sintered density, and the mechanical properties of the sintered samples.</li> </ol>
[49]	WC-9Co	Solid loading, printing temperature, microfilament overlap ratio, printing layer thickness, debinding and sintering processes	<ol style="list-style-type: none"> <li>A WC-9Co cemented-carbide green body, free of printed defects and possessing a relative density of 98.5%, was fabricated via MEX at a printing temperature of 150 °C, with a microfilament overlap ratio of 30% and a printing layer thickness of 0.1 mm.</li> <li>The WC-9Co cemented carbide, prepared through two-step solvent debinding followed by continuous thermal debinding and vacuum pressure sintering, displays a uniform microstructure comprising two phases: WC and Co. It also features small average-sized WC grains that are uniformly distributed.</li> </ol>
[50]	WC-8Co	Debinding and sintering atmosphere, sintering temperature	<ol style="list-style-type: none"> <li>Thermal debinding in vacuum and argon atmospheres results in uncombined carbon formation.</li> <li>Sintering under hydrogen and vacuum effectively promotes further decomposition and transformation of residual carbon, whereas sintering in an argon atmosphere causes uncombined carbon aggregation.</li> <li>Excessively high sintering temperatures lead to WC grain growth, which can deteriorate the mechanical properties of the sintered body.</li> </ol>
[51]	WC-8Co	Water-soluble binder, debinding process, comparison of 3DGP vs. conventional process	<ol style="list-style-type: none"> <li>Residual carbon and decarburization during thermal debinding can be minimized by employing a N<sub>2</sub>/H<sub>2</sub> atmosphere in the furnace.</li> <li>The completely debound body achieves near-full densification when sintered above 1340 °C.</li> <li>Carbides processed via 3DGP exhibit slightly inferior properties compared to those produced by conventional powder metallurgy processes.</li> </ol>

### 3. Testing Methods for AM-Processed Cemented Carbides

The testing methods for AM-processed cemented carbides are largely analogous to those for traditionally processed ones. Per ASTM B311-17 [52], the green density and post-sintering density of printed cemented carbide parts can be measured using the Archimedean drainage method [36]. Additionally, an X-ray micro-CT can be utilized to directly assess the porosity (and indirectly the relative density) of AM-processed carbides [20]. As referenced in [41], the Rockwell A hardness of AM-processed carbides can be determined. The microhardness can be evaluated using the Vickers scale for a range of loads according to ISO 6507 [53]. The transverse rupture strength of cemented carbides can be readily determined according to ISO 3327 [54]. Additionally, a more precise method for measuring transverse rupture strength is provided by ASTM B406 [55]. The Palmquist method (ISO 28079) [56] is a commonly used method for assessing the fracture toughness of AM-processed carbides, though its accuracy is debatable despite its simplicity. The wear properties of cemented carbide samples are evaluated according to ASTM B611 [40] and ASTM G65 [41] procedures.

## 4. Discussion

### 4.1. Challenges, Solutions, and Future Directions of SLM/LPBF

The SLM process frequently induces cracks and warpings in cemented carbides. Furthermore, abnormal WC grain growth, WC decomposition, and the formation of low-carbon phases are commonly observed. These defects primarily arise from the extremely high local sintering temperature, exceedingly brief sintering time, and non-uniform thermal distribution inherent in the SLM process. Additionally, Co evaporation and carbon loss are major issues that compromise the fracture toughness and transverse rupture strength of carbides. Although the loss of Co and carbon may enhance the wear resistance to some extent, the resultant decrease in toughness is a critical concern. This directly affects a material's capacity to endure the rigorous conditions encountered in various industrial applications.

To address these challenges, researchers have been focusing on optimizing the SLM parameters to minimize thermal gradients and reduce the associated residual stresses. This optimization includes the augmentation of the baseplate preheating temperature, as well as the fine-tuning of the laser power, scanning speed, and hatch spacing to achieve a more uniform heat distribution and improve the densification of the molten pool. In addition, the feedstock carbide powder material design can be made to compensate for the Co loss. Moreover, a sintering treatment after SLM processing is necessary to remove thermal cracking, reduce the low-carbon phases, and improve the microstructure quality. By adopting these methods, the formation of cracks and warpings can be reduced to some degree, leading to an enhancement of the mechanical properties and overall quality of SLM-manufactured carbides.

The pursuit of these optimization strategies is essential for the advancement of the SLM technique in the production of high-performance cemented carbides that can meet the stringent requirements of modern engineering applications. Owing to the distinctive attributes of Selective Laser Melting (SLM), it appears more judicious to employ this technique for the fabrication of carbides with elevated cobalt (Co) concentrations. A greater investment of research efforts is warranted in this specific area.

### 4.2. Challenges, Solutions, and Future Directions of SEBM

The production of cemented carbide samples through SEBM often results in structures that incorporate layers with medium-coarse and abnormally large WC grains, presenting a considerable challenge for additive manufacturing processes. These microstructural characteristics can lead to inconsistencies in the material properties and potential weaknesses

of the final product. Furthermore, cemented carbide articles fabricated using SEBM are commonly marked by a high surface roughness, particularly on the side surfaces. This high surface roughness is a critical factor that can impede the functional performance and aesthetic appeal of the components, especially in applications where precision and smoothness are required.

Consequently, there is a compelling need for the development and implementation of specialized heat treatment techniques tailored for carbide articles with intricate geometries that are derived from SEBM processes. These treatments include liquid-phase sintering and a surface treatment process post-SEBM process. Liquid-phase sintering is necessary to adjust the residual stress and enhance the microstructure quality. A surface treatment is essential not only for improving the surface finish but also for enhancing the mechanical integrity and performance of the carbide components. Surface treatment methods can include, but are not limited to, thermal etching, abrasive blasting, and chemical polishing, each of which can address the surface roughness and achieve the desired level of refinement. By refining the surface, these treatments can also help to reduce the potential stress concentration areas that might initiate cracks or an early failure in service.

In comparison to SLM, SEBM demonstrates superior efficiency and enhanced control over residual stresses, making it a more fitting choice for the production of carbides with larger dimensions. Conversely, the considerably high energy of the electron beam complicates the precise regulation of sintering temperatures. As such, carbides with a higher metal content and larger dimensions are better suited for the SEBM process. A greater emphasis on the research and development of this material category is essential to fully capitalize on the technical advantages offered by the SEBM process.

#### *4.3. Challenges, Solutions, and Future Directions of SLS*

Achieving a high relative density is a formidable challenge in the SLS processing of carbides, even with the employment of sophisticated sintering techniques and infiltration strategies. This limitation significantly undermines the feasibility of the SLS process for the additive manufacturing of cemented carbides, as attaining full density is imperative for a material's performance and structural integrity. The sintering process, which aims to coalesce particles and eliminate porosity, often proves inadequate in SLS when compared with other AM techniques such as SLM. The infiltration step, designed to fill residual porosity with a secondary material, can also be ineffectual for achieving the requisite density levels. Consequently, this leads to suboptimal mechanical properties of the final product, such as reduced strength, toughness, and wear resistance.

To overcome these challenges and unlock the full potential of SLS in the additive manufacturing domain for carbide materials, an advanced feedstock carbide powder material design is required to minimize the organic binder size and enhance the sintering/infiltration characteristics. Additionally, post-processing techniques, such as hot isostatic pressing (HIP), could be employed to further densify the sintered parts and improve their mechanical properties.

#### *4.4. Challenges, Solutions, and Future Directions of BJAM*

When compared with the results obtained from SLM, SEBM, and SLS, the carbides processed via BJAM exhibit markedly superior densification, enhanced microstructure quality, and, as a consequence, improved mechanical properties. The capacity of the BJAM process to yield carbides with these enhanced attributes confers a significant advantage for applications that demand high strength and durability. However, the BJAM process is not without its attendant challenges.

Notably, significant geometric distortion and suboptimal surface quality are frequently observed following the sintering phase, primarily due to the considerable shrinkage during this critical stage. These issues pose substantial hurdles for the BJ processing of complex-shaped carbides, where a precise dimensional control and surface finish are of paramount importance. Furthermore, the occurrence of abnormal tungsten carbide (WC) grain growth and the aggregation of coarse WC grains upon sintering have been well documented in BJ-processed cemented carbides. Such microstructural anomalies can compromise a material's mechanical properties, including its strength and toughness, thereby negatively impacting the service performance of the carbides in practical applications.

To ameliorate these effects and optimize the BJAM process for carbide production, there is an imperative need for intensified research endeavors on feedstock carbide powder material design, printing process optimization, and treatments post-printing process. The focus should be squarely on developing robust strategies to control WC grain growth, minimize dimensional shrinkage, and enhance the surface quality of the sintered parts. This could entail refining the feedstock carbide formulation to achieve a more uniform particle distribution and size, optimizing the sintering parameters to better manage the thermal dynamics of the process, or exploring advanced post-processing techniques, such as heat treatment or surface-finishing methods, to mitigate microstructural irregularities and improve dimensional accuracy.

Addressing these challenges is not only essential but also urgent to fully harness the potential of BJAM in the manufacturing of high-performance cemented carbides. By overcoming these obstacles, the BJAM process could be refined to produce carbides that meet the stringent demands of modern industries, thereby expanding its applicability to sectors where high-strength, durable materials are indispensable for the advancement of technological innovations and the enhancement of industrial productivity.

#### *4.5. Challenges, Solutions, and Future Directions of 3DGP*

The 3DGP process typically employs a significantly finer grade of feedstock carbide powders than the SLM, SEBM, SLS, and BJ processes. This key difference confers superior sintering performance to the carbides processed via 3DGP, enabling them to surpass the sintering quality attainable through other AM techniques. However, the dimensional accuracy and geometric precision of the carbides produced by the 3DGP process are largely determined by the nozzle size utilized. This often results in lower dimensional precision compared to other AM technologies, thereby rendering the 3DGP process less accurate in terms of the final product's dimensions and geometry.

Moreover, the printing efficiency of the 3DGP process is generally deemed to be suboptimal. This inefficiency poses a considerable challenge that warrants attention and improvement. To surmount these limitations, extensive research efforts are imperative. It is crucial to allocate resources to further studies aimed at rectifying the existing deficiencies of the 3DGP process. The objective should be to enhance its precision, efficiency, and overall performance within the spectrum of AM technologies. By doing so, the 3DGP process could be optimized to better meet the demands of high-precision and high-efficiency manufacturing, thereby expanding its applicability and competitiveness in the field of advanced materials fabrication.

#### *4.6. Comparison of Different AM Techniques*

In conclusion, cemented carbides synthesized using BJAM or 3DGP processes are more likely to achieve high density, high hardness, and exceptional fracture toughness, which are comparable to those of samples prepared using conventional methods. Conversely, WC-Co carbides produced through SLM and SEBM processes display increased hardness

but reduced strength and fracture toughness. This discrepancy is attributed to the uneven heat distribution characteristic of the selective melting processes, particularly in SLM, which can result in cobalt evaporation and the formation of ternary phases. These factors are known to enhance hardness but also increase brittleness. Additionally, the presence of cracks and uneven microstructures further reduce the strength and fracture toughness of these materials.

A comprehensive compilation of the mechanical properties of additively manufactured WC-Co carbides, as reported in the literature, is detailed in Table 8. This table serves as a summary for comparing the performance of different additive manufacturing techniques in the context of WC-Co carbides, highlighting the nuances in the material properties that arise from variations in the processing methods.

**Table 8.** Mechanical properties of WC-Co carbides fabricated by different AM methods.

Process	Material	Powder Parameters	Relative Density (%)	Hardness	Fracture Toughness (MPa $\sqrt{m}$ )	Ref.
SLM	WC-17Co	Spherical carbide granules	96.2	9.0–9.5 GPa	N/A	[18]
	CC-NiAlCoCrCuFe	Spherical cast carbide: 27.69 $\mu\text{m}$	99.36	711.7–1178.6 HV1 in low-W content area; 1306.8–1413.4 HV1 in high-W content area	9.74–13.29	[19]
	WC-12Co	Spherical carbide granule: 13.74 $\mu\text{m}$	98.7–99.6	1260–1320 HV30	$\geq 17.4$	[20]
SEBM	WC-13Co	Irregular-shaped WC-13Co granule: 60–100 $\mu\text{m}$	N/A	9.0–9.5 GPa	about 20	[25]
	WC-12Co	Spherical WC-12Co granule: 84 $\mu\text{m}$	N/A	18.92 GPa	N/A	[26]
SLS	WC-9Co, WC-50Co, WC-18Cu-12Co with bronze infiltration	WC: <45 $\mu\text{m}$	76–96	26–155 HB	N/A	[28]
	WC-12Co	Spherical WC-12Co granule: 34 $\mu\text{m}$	65	N/A	N/A	[30]
BJAM	WC-12Co	Spherical WC-12Co granule: 25.16 $\mu\text{m}$	98.4	88.9 HRA or 1256 HV30	17	[36]
	WC (infiltration 32 vol.% of Co)	WC: 19.21 $\mu\text{m}$	98.5	9.0 GPa	23.2	[46]
	WC (infiltration 35.6 vol.% of Co)	WC: 19.2 $\mu\text{m}$	>97	9.32–11.2 GPa	25.87	[45]
	WC-10Co and WC-12Co	Spherical WC-10Co granule: 20.3 $\mu\text{m}$ ; Spherical WC-12Co granule: 21.2 $\mu\text{m}$	100	WC-10Co: 1119 HV30; WC-12Co: 1050 HV30	WC-10Co: 18.8; WC-12Co: 19.4	[42]
	WC-10-17Co	Spherical WC-Co granules: 19.5–25.2 $\mu\text{m}$	99–99.7	WC (extra coarse)-10Co: 1058 HV30; WC (extra coarse)-12Co: 993–1050 HV30; WC (medium)-12Co: 1203–1306 HV30; WC (medium coarse)-17Co: 1067 HV30	WC (extra coarse)-10Co: 18.8; WC (extra coarse)-12Co: $\geq 19.4$ ; WC (medium)-12Co: 17–23; WC (medium coarse)-17Co: N/A	[43]
	WC-8Co	WC-Co composite powder: 3.4 $\mu\text{m}$	99.8	90 HRA	N/A	[48]
	WC-9Co	WC-Co composite powder	99.7	1525 HV30	20.4	[49]
3DGP	WC-20Co	WC: 2.7 $\mu\text{m}$ ; Co: 46.5 $\mu\text{m}$	99.93	87.7 HRA	N/A	[47]

## 5. Summary

This study provides a concise overview of the current research landscape concerning the additive manufacturing of cemented carbides, with a focus on both direct and indirect AM processes. It has been observed that each category of AM processes possesses its own set of advantages and disadvantages when it comes to the fabrication of cemented carbides. The significant challenges posed by these techniques impede the rapid advancement of AM-processed carbides for diverse applications. The following conclusions have been drawn:

- (1) Additive manufacturing has emerged as a viable method for producing WC-Co carbides, yielding mechanical properties that are generally comparable to those of conventionally manufactured materials. However, AM also introduces unique manufacturing challenges that necessitate further investigation.
- (2) In the context of SLM and SEBM, printing and sintering are performed in a single, integrated step. Nevertheless, non-uniform heating, significant temperature gradients, and extremely high heating and cooling rates often result in uneven sintering, the decomposition of WC grains, and frequent cracking post-solidification, thereby diminishing the mechanical properties. Additional sintering following the SLM/SEBM process can enhance the density and microstructure quality to some extent, but it is insufficient to resolve all the associated issues.
- (3) SLS faces notable difficulties in achieving a high relative density of carbides. BJAM produces WC-Co samples with a reduced incidence of cracking, but is not without its drawbacks, such as abnormal WC grain growth, coarse WC clustering, Co pool formation, and porosity. Three-dimensional gel-printing offers certain advantages in terms of the sintering performance, but dimensional and geometric precision control, as well as fabrication efficiency, remain its primary limitations. Cemented carbides produced using these indirect-forming AM processes have yet to match the quality of their traditionally prepared counterparts.
- (4) A comprehensive investigation into the densification–microstructure evolution mechanisms, taking into account the unique characteristics of AM processing, is of paramount importance for the development of AM processes and the enhancement of the mechanical properties of cemented carbides. Such research is essential to overcome the current challenges and to fully realize the potential of AM for the production of high-performance cemented carbides.

## 6. Future Directions

For direct-forming techniques, such as SLM and SEBM, achieving precise control over the temperature and sintering time presents a considerable challenge. This often leads to overburning or under-sintering, which in turn impedes the development of an optimal microstructure. Consequently, a comprehensive optimization of the post-printing sintering treatment has become increasingly imperative for the SLM/SEBM processing of carbides.

Indirect AM techniques, including SLS, BJAM, and 3DGP, hold great promise for the manufacturing of cemented carbides. These methods capitalize on traditional sintering processes and offer enhanced control over the microstructure of the final product. However, these techniques also face significant hurdles to improving density and microstructure quality. The design of the feedstock powder material may be pivotal for overcoming these challenges.

Despite the inherent potential of these AM technologies, further research is indispensable to refine the material design, optimize the printing processes, explore debinding–sintering procedures, characterize microstructures, and evaluate mechanical properties. Progress in these areas will be crucial for enhancing the capabilities and quality of AM-produced cemented carbides. Ensuring their competitiveness with traditionally manu-

factured carbides, in terms of their microstructure quality, efficiency, performance, and reliability, will depend on such advancements.

**Author Contributions:** Conceptualization, Z.Z.; Investigation, X.N. and Z.H.; Data curation, W.Y.; Funding acquisition, X.D.; Methodology, S.W. and Y.L.; Project administration, X.D. and J.L.; Resources, G.N., H.W. and Y.H.; Supervision, G.N.; Writing—original draft, Z.Z.; Writing—review and editing, J.L. All authors have read and agreed to the published version of the manuscript.

**Funding:** This research was funded by the Foshan Science and Technology Innovation Team project (FS0AA-KJ919-4402-0023) and Yangjiang Innovation Research Team Introduction Project (Grant No. RCZX2024003).

**Data Availability Statement:** The dataset, integral to our ongoing research, is available for scholarly dissemination upon formal request to the corresponding author(s).

**Acknowledgments:** The authors appreciate the financial support from the Foshan Science and Technology Innovation Team project (FS0AA-KJ919-4402-0023) and Yangjiang Innovation Research Team Introduction Project (Grant No. RCZX2024003).

**Conflicts of Interest:** Authors Xin Deng, Shanghua Wu, Yanhui Li, Guanglin Nie, Haidong Wu and Jinyang Liu were employed by the company Guangdong Metal Ceramic 3D Technology Co., Ltd. Author Yong Huang was employed by the company Guangzhou Dupo Scientific Instrument Co., Ltd. The remaining authors declare that the research was conducted in the absence of any commercial or financial relationships that could be construed as a potential conflict of interest.

## References

1. Fang, Z.Z.; Koopman, M.C.; Wang, H. Cemented Tungsten Carbide Hardmetal—An Introduction. *Compr. Hard Mater.* **2014**, *1*, 123–137. [[CrossRef](#)]
2. Chen, C.; Huang, B.; Liu, Z.; Li, Y.; Zou, D.; Liu, T.; Chang, Y.; Chen, L. Additive manufacturing of WC-Co cemented carbides: Process, microstructure, and mechanical properties. *Addit. Manuf.* **2023**, *63*, 103410. [[CrossRef](#)]
3. Li, X.; Zhao, Y.; Guo, Z.; Liu, Y.; Wang, H.; Zhang, J.; Yi, D.; Cao, Y.; Yang, X.; Liu, B.; et al. Influence of different substrates on the microstructure and mechanical properties of WC-12Co cemented carbide fabricated via laser melting deposition. *Int. J. Refract. Met. Hard Mater.* **2022**, *104*, 105787. [[CrossRef](#)]
4. Xiong, Y.; Smugeresky, J.E.; Ajdelsztajn, L.; Schoenung, J.M. Fabrication of WC-Co cermets by laser engineered net shaping. *Mater. Sci. Eng. A* **2008**, *493*, 261–266. [[CrossRef](#)]
5. García, J.; Ciprés, V.C.; Blomqvist, A.; Kaplan, B. Cemented Carbide Microstructures: A Review. *Int. J. Refract. Met. Hard Mater.* **2019**, *80*, 40–68. [[CrossRef](#)]
6. Ortner, H.M.; Ettmayer, P.; Kolaska, H.; Smid, I. The History of the Technological Progress of Hardmetals. *Int. J. Refract. Met. Hard Mater.* **2015**, *44*, 3–8. [[CrossRef](#)]
7. Yang, Y.; Zhang, C.; Wang, D.; Nie, L.; Wellmann, D.; Tian, Y. Additive Manufacturing of WC-Co Hardmetals: A Review. *Int. J. Adv. Manuf. Technol.* **2020**, *108*, 1653–1673. [[CrossRef](#)]
8. Upadhyaya, G.S. Materials Science of Cemented Carbides—An Overview. *Mater. Des.* **2001**, *22*, 483–489. [[CrossRef](#)]
9. Su, W.; Sun, Y.; Wang, H.; Zhang, X.; Ruan, J. Preparation and sintering of WC-Co composite powders for coarse grained WC-8Co hardmetals. *Int. J. Refract. Met. Hard Mater.* **2014**, *45*, 80–85. [[CrossRef](#)]
10. Emani, S.V.; Santos, A.F.R.D.; Shaw, L.L.; Chen, Z. Investigation of Microstructure and Mechanical Properties at Low and High Temperatures of WC-6 wt.% Co. *Int. J. Refract. Met. Hard Mater.* **2016**, *58*, 172–181. [[CrossRef](#)]
11. Thompson, S.M.; Bian, L.; Shamsaei, N.; Yadollahi, A. An overview of direct laser deposition for additive manufacturing; Part I: Transport phenomena, modeling and diagnostics. *Addit. Manuf.* **2015**, *8*, 36–62. [[CrossRef](#)]
12. Kruth, J.; Mercelis, P.; Van Vaerenbergh, J.; Froyen, L.; Rombouts, M. Binding mechanisms in selective laser sintering and selective laser melting. *Rapid Prototyp. J.* **2005**, *11*, 26–36. [[CrossRef](#)]
13. Chen, J.; Huang, M.; Fang, Z.Z.; Koopman, M.; Liu, W.; Deng, X.; Zhao, Z.; Chen, S.; Wu, S.; Liu, J.; et al. Microstructure Analysis of High Density WC-Co Composite Prepared by One Step Selective Laser Melting. *Int. J. Refract. Met. Hard Mater.* **2019**, *84*, 104980. [[CrossRef](#)]
14. Domashenkov, A.; Borbély, A.; Smurov, I. Structural modifications of WC-Co nanophased and conventional powders processed by selective laser melting. *Mater. Manuf. Process.* **2017**, *32*, 93–100. [[CrossRef](#)]

15. Grigoriev, S.; Tarasova, T.; Gusarov, A.; Khmyrov, R.; Egorov, S. Possibilities of Manufacturing Products from Cermet Compositions Using Nanoscale Powders by Additive Manufacturing Methods. *Materials* **2019**, *12*, 3425. [[CrossRef](#)] [[PubMed](#)]
16. Liu, J.; Chen, J.; Zhou, L.; Liu, B.; Lu, Y.; Wu, S.; Deng, X.; Lu, Z.; Xie, Z.; Liu, W.; et al. Role of Co Content on Densification and Microstructure of WC–Co Cemented Carbides Prepared by Selective Laser Melting. *Acta Metall. Sin. (Engl. Lett.)* **2021**, *34*, 1245–1254. [[CrossRef](#)]
17. Khmyrov, R.S.; Safronov, V.A.; Gusarov, A.V. Synthesis of Nanostructured WC-Co Hardmetal by Selective Laser Melting. *Mater. Sci. Forum* **2015**, *834*, 77–83. [[CrossRef](#)]
18. Uhlmann, E.; Bergmann, A.; Gridin, W. Investigation on Additive Manufacturing of Tungsten Carbide-Cobalt by Selective Laser Melting. *Procedia CIRP* **2015**, *35*, 8–15. [[CrossRef](#)]
19. Li, C.-W.; Chang, K.C.; Yeh, A.C. On the Microstructure and Properties of an Advanced Cemented Carbide System Processed by Selective Laser Melting. *J. Alloys Compd.* **2019**, *782*, 440–450. [[CrossRef](#)]
20. Xing, M.; Wang, H.; Zhao, Z.; Lu, H.; Liu, C.; Lin, L.; Wang, M.; Song, X. Additive manufacturing of cemented carbides inserts with high mechanical performance. *Mater. Sci. Eng. A* **2022**, *861*, 144350. [[CrossRef](#)]
21. Gu, D.D.; Wilhelm, M. Microstructure Characteristics and Formation Mechanisms of In Situ WC Cemented Carbide Based Hardmetals Prepared by Selective Laser Melting. *Mater. Sci. Eng. A* **2010**, *527*, 7585–7592. [[CrossRef](#)]
22. Ergüder, T.O.; Güler, O.; Yıldız, F. Determination of selective laser melting process parameters of tungsten carbide powders coated with nickel via electroless plating for improved interface properties. *Int. J. Refract. Met. Hard Mater.* **2024**, *122*, 106735. [[CrossRef](#)]
23. Sochalski-Kolbus, L.M.; Payzant, E.A.; Cornwell, P.A.; Watkins, T.R.; Babu, S.S.; Dehoff, R.R.; Lorenz, M.; Ovchinnikova, O.; Duty, C. Comparison of residual stresses in Inconel 718 simple parts made by electron beam melting and direct laser metal sintering. *Metall. Mater. Trans. A* **2015**, *46*, 1419–1432. [[CrossRef](#)]
24. Peng, H.; Liu, C.; Guo, H.; Yuan, Y.; Gong, S.; Xu, H. Fabrication of WCp/NiBSi Metal Matrix Composites by Electron Beam Melting. *Mater. Sci. Eng. A* **2016**, *666*, 320–323. [[CrossRef](#)]
25. Konyashin, I.; Hinners, H.; Ries, B.; Kirchner, A.; Klöden, B.; Kieback, B.; Nilen, R.; Sidorenko, D. Additive Manufacturing of WC-13%Co by Selective Electron Beam Melting: Achievements and Challenges. *Int. J. Refract. Met. Hard Mater.* **2019**, *84*, 105028. [[CrossRef](#)]
26. Wang, J.; Han, Y.; Zhao, Y.; Li, X.; Yi, D.; Guo, Z.; Cao, Y.; Liu, B.; Tang, H. Microstructure and Properties of WC-12Co Cemented Carbide Fabricated via Selective Electron Beam Melting. *Int. J. Refract. Met. Hard Mater.* **2022**, *106*, 105847. [[CrossRef](#)]
27. Kumar, S. Process chain development for additive manufacturing of cemented carbide. *J. Manuf. Process.* **2018**, *34*, 121–130. [[CrossRef](#)]
28. Kumar, S. Manufacturing of WC-Co Moulds Using SLS Machine. *J. Mater. Process. Technol.* **2008**, *209*, 3840–3848. [[CrossRef](#)]
29. Kumar, S.; Czekanski, A. Optimization of parameters for SLS of WC-Co. *Rapid Prototyp. J.* **2017**, *23*, 1202–1211. [[CrossRef](#)]
30. Jucan, O.D.; Gadalean, R.V.; Chicinas, H.F.; Hering, M.; Balc, N.; Popa, C.O. Study on the Indirect Selective Laser Sintering (SLS) of WC-Co/PA12 Powders for the Manufacturing of Cemented Carbide Parts. *Int. J. Refract. Met. Hard Mater.* **2021**, *96*, 105498. [[CrossRef](#)]
31. Gădălean, R.V.; Jucan, O.D.; Chicinas, H.F.; Balc, N.; Popa, C.O. Additive Manufacturing of WC-Co by Indirect Selective Laser Sintering (SLS) using High Bulk Density Powders. *Arch. Metall. Mater.* **2022**, *67*, 577–585. [[CrossRef](#)]
32. Berman, B. 3-D Printing: The New Industrial Revolution. *Bus. Horiz.* **2012**, *55*, 155–162. [[CrossRef](#)]
33. Do, T.; Kwon, P.; Shin, C.S. Process development toward full-density stainless steel parts with binder jetting printing. *Int. J. Refract. Met. Hard Mater.* **2017**, *121*, 50–60. [[CrossRef](#)]
34. Enneti, R.K.; Prough, K.C. Effect of Binder Saturation and Powder Layer Thickness on the Green Strength of the Binder Jet 3D Printing (BJ3DP) WC-12%Co Powders. *Int. J. Refract. Met. Hard Mater.* **2019**, *84*, 104991. [[CrossRef](#)]
35. Mostafaei, A.; De Vecchis, P.R.; Kimes, K.A.; Elhassid, D.; Chmielus, M. Effect of Binder Saturation and Drying Time on Microstructure and Resulting Properties of Sinter-HIP Binder-Jet 3D-Printed WC-Co Composites. *Addit. Manuf.* **2021**, *46*, 102128. [[CrossRef](#)]
36. Mariani, M.; Goncharov, I.; Mariani, D.; De Gaudenzi, G.P.; Popovich, A.; Lecis, N.; Vedani, M. Mechanical and Microstructural Characterization of WC-Co Consolidated by Binder Jetting Additive Manufacturing. *Int. J. Refract. Met. Hard Mater.* **2021**, *100*, 105639. [[CrossRef](#)]
37. Kumar, K.C.; Ramalingam, M.S.; Joshi, S.S.; Sharma, S.; Dahotre, N.B. Role of powder morphology in liquid phase sintering of binder jet additively fabricated WC–Co composite. *Addit. Manuf.* **2024**, *95*, 104520. [[CrossRef](#)]
38. Enneti, R.K.; Prough, K.C.; Wolfe, T.A.; Klein, A.; Studley, N.; Trasorras, J.L. Sintering of WC-12%Co Processed by Binder Jet 3D Printing (BJ3DP) Technology. *Int. J. Refract. Met. Hard Mater.* **2018**, *71*, 28–35. [[CrossRef](#)]
39. Enneti, R.K.; Prough, K.C. Wear Properties of Sintered WC-12%Co Processed via Binder Jet 3D Printing (BJ3DP). *Int. J. Refract. Met. Hard Mater.* **2019**, *78*, 228–232. [[CrossRef](#)]

40. ASTM B611-21; Standard Test Method for Determining the High Stress Abrasion Resistance of Hard Materials. ASTM International: West Conshohocken, PA, USA, 2021.
41. ASTM G65-16; Standard Test Method for Measuring Abrasion Using the Dry Sand/Rubber Wheel Apparatus. ASTM International: West Conshohocken, PA, USA, 2021.
42. Wolfe, T.; Shah, R.; Prough, K.; Trasorras, J.L. Coarse Cemented Carbide Produced via Binder Jetting 3D Printing. *Int. J. Refract. Met. Hard Mater.* **2023**, *110*, 106016. [[CrossRef](#)]
43. Wolfe, T.A.; Shah, R.M.; Prough, K.C.; Trasorras, J.L. Binder jetting 3D printed cemented carbide: Mechanical and wear properties of medium and coarse grades. *Int. J. Refract. Met. Hard Mater.* **2023**, *113*, 106197. [[CrossRef](#)]
44. Cramer, C.L.; Aguirre, T.G.; Wieber, N.R.; Lowden, R.A.; Trofimov, A.A.; Wang, H.; Yan, J.; Paranthaman, M.P.; Elliott, A.M. Binder Jet Printed WC Infiltrated with Pre-made Melt of WC and Co. *Int. J. Refract. Met. Hard Mater.* **2020**, *87*, 105137. [[CrossRef](#)]
45. Cramer, C.L.; Wieber, N.R.; Aguirre, T.G.; Lowden, R.A.; Elliott, A.M. Shape Retention and Infiltration Height in Complex WC-Co Parts Made via Binder Jet of WC with Subsequent Co Melt Infiltration. *Addit. Manuf.* **2019**, *29*, 100828. [[CrossRef](#)]
46. Cramer, C.L.; Nandwana, P.; Lowden, R.A.; Elliott, A.M. Infiltration Studies of Additive Manufacture of WC with Co Using Binder Jetting and Pressureless Melt Method. *Addit. Manuf.* **2019**, *28*, 333–343. [[CrossRef](#)]
47. Zhang, X.; Guo, Z.; Chen, C.; Yang, W. Additive Manufacturing of WC-20Co Components by 3D Gel-Printing. *Int. J. Refract. Met. Hard Mater.* **2018**, *70*, 215–223. [[CrossRef](#)]
48. Li, Y.; Guo, Z. Gelcasting of WC-8wt%Co Tungsten Cemented Carbide. *Int. J. Refract. Met. Hard Mater.* **2008**, *26*, 472–477. [[CrossRef](#)]
49. Chen, C.; Huang, B.; Liu, Z.; Chen, L.; Li, Y.; Zou, D.; Chang, Y.; Cheng, X.; Zhou, R.; Liu, Y. Material extrusion additive manufacturing of WC-9Co cemented carbide. *Addit. Manuf.* **2024**, *86*, 104203. [[CrossRef](#)]
50. Zhao, Z.; Liu, R.; Chen, J.; Xiong, X. Carbon control and densification of WC-8%Co fabricated by extrusion-based additive manufacturing under pressureless sintering. *Mater. Today Commun.* **2023**, *36*, 106866. [[CrossRef](#)]
51. Zhao, Z.; Liu, R.; Chen, J.; Xiong, X. Material extrusion printing of WC-8%Co cemented carbide based on partly water-soluble binder and post-processing. *J. Mater. Res. Technol.* **2024**, *29*, 4394–4405. [[CrossRef](#)]
52. ASTM B311-17; Standard Test Method for Density of Powder Metallurgy (PM) Materials Containing Less Than Two Percent Porosity. ASTM International: West Conshohocken, PA, USA, 2017.
53. ISO 6507-1:2018; Metallic Materials—Vickers Hardness Test—Part 1: Test Method. International Organization for Standardization (ISO): Geneva, Switzerland, 2018.
54. ISO 3327:2009; Hardmetals—Determination of Transverse Rupture Strength. International Organization for Standardization (ISO): Geneva, Switzerland, 2009.
55. ASTM B406-96 (Reapproved 2021); Standard Test Method for Transverse Rupture Strength of Cemented Carbides. ASTM International: West Conshohocken, PA, USA, 2021. [[CrossRef](#)]
56. ISO 28079:2009; Hardmetals—Palmqvist Toughness Test. International Organization for Standardization (ISO): Geneva, Switzerland, 2009.

**Disclaimer/Publisher’s Note:** The statements, opinions and data contained in all publications are solely those of the individual author(s) and contributor(s) and not of MDPI and/or the editor(s). MDPI and/or the editor(s) disclaim responsibility for any injury to people or property resulting from any ideas, methods, instructions or products referred to in the content.